

# 2D Materials Nanoarchitectonics for 3D Structures/Functions

Katsuhiko Ariga <sup>1,2</sup> 

<sup>1</sup> Research Center for Materials Nanoarchitectonics (MANA), National Institute for Materials Science (NIMS), 1-1 Namiki, Tsukuba 305-0044, Ibaraki, Japan; ariga.katsuhiko@nims.go.jp

<sup>2</sup> Graduate School of Frontier Sciences, The University of Tokyo, 5-1-5 Kashiwanoha, Kashiwa 277-8561, Chiba, Japan

**Abstract:** It has become clear that superior material functions are derived from precisely controlled nanostructures. This has been greatly accelerated by the development of nanotechnology. The next step is to assemble materials with knowledge of their nano-level structures. This task is assigned to the post-nanotechnology concept of nanoarchitectonics. However, nanoarchitectonics, which creates intricate three-dimensional functional structures, is not always easy. Two-dimensional nanoarchitectonics based on reactions and arrangements at the surface may be an easier target to tackle. A better methodology would be to define a two-dimensional structure and then develop it into a three-dimensional structure and function. According to these backgrounds, this review paper is organized as follows. The introduction is followed by a summary of the three issues; (i) 2D to 3D dynamic structure control: liquid crystal commanded by the surface, (ii) 2D to 3D rational construction: a metal–organic framework (MOF) and a covalent organic framework (COF); (iii) 2D to 3D functional amplification: cells regulated by the surface. In addition, this review summarizes the important aspects of the ultimate three-dimensional nanoarchitectonics as a perspective. The goal of this paper is to establish an integrated concept of functional material creation by reconsidering various reported cases from the viewpoint of nanoarchitectonics, where nanoarchitectonics can be regarded as a method for everything in materials science.

**Keywords:** covalent organic framework (COF); liquid crystal; living cell; metal–organic framework (MOF); nanoarchitectonics; surface; three dimensions; two dimensions



**Citation:** Ariga, K. 2D Materials Nanoarchitectonics for 3D Structures/Functions. *Materials* **2024**, *17*, 936. <https://doi.org/10.3390/ma17040936>

Academic Editors: Gueorgui Gueorguiev and Toma Stoica

Received: 20 January 2024  
Revised: 9 February 2024  
Accepted: 9 February 2024  
Published: 17 February 2024



**Copyright:** © 2024 by the author. Licensee MDPI, Basel, Switzerland. This article is an open access article distributed under the terms and conditions of the Creative Commons Attribution (CC BY) license (<https://creativecommons.org/licenses/by/4.0/>).

## 1. Introduction

The development of new technologies such as information technology, device technology, and medical technology is supporting the development of society. However, materials chemistry, which has been steadily developing since the 20th century, is also indispensable [1,2]. Useful materials are essential to fulfill important parts of the later technologies. Such developments in materials chemistry solve a variety of existing problems. Energy production [3–18], energy storage [19–30], environmental remediation [31–40], carbon neutral strategies [41–46], detection of hazardous substances [47–52], bio-related sensing [53–58], technologies leading to medicine [59–69], and the creation of device materials to support them [70–75] are among the many demands that depend on the development of materials chemistry. Effective function is not determined solely by the properties of the substances themselves. Their functions depend much on what kind of structure a substance takes or what kind of internal structure it takes. With the progress of materials chemistry, such matters have been gradually elucidated. This has been greatly accelerated by the development of nanotechnology. As is still the case in current research, nanotechnology makes it possible to observe nanostructures from the atomic and molecular levels [76–89]. Accordingly, it has become clear that superior material functions are derived from precisely controlled nanostructures. The next step is to assemble materials with knowledge of their nano-level structures. This task is assigned to the post-nanotechnology concept of nanoarchitectonics (Figure 1) [90].

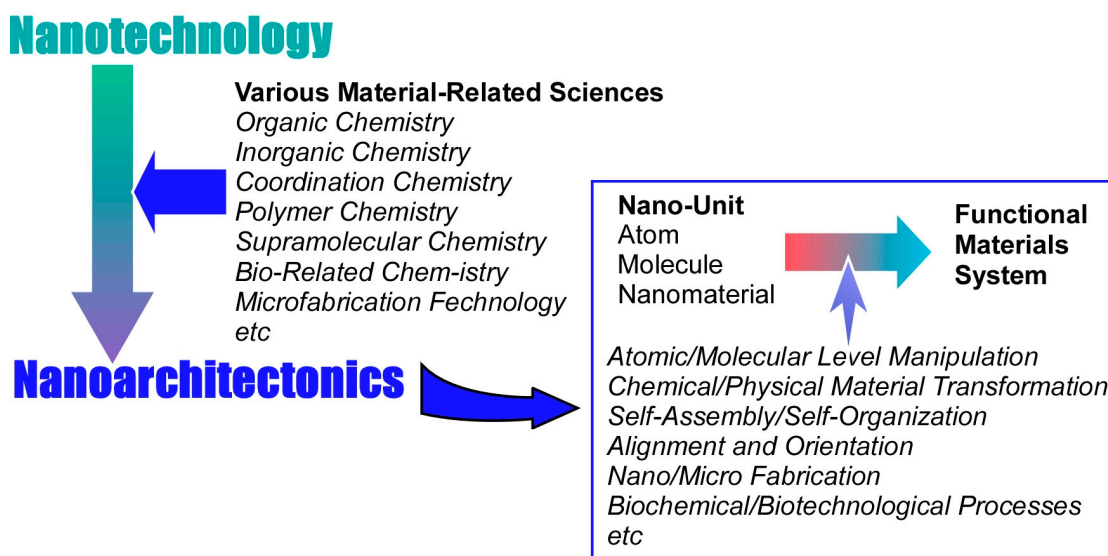


**Figure 1.** Outline of the nanoarchitectonics concept which establishes a methodology for building functional material systems from nano-units such as atoms, molecules, and nanomaterials.

Nanotechnology was founded by Richard Feynman in the middle of the 20th century [91,92]. In the early 21st century, nanoarchitectonics was proposed by Masakazu Aono [93,94] as a successor to Feynman's work. The goal of nanoarchitectonics is to establish a methodology for building functional material systems from nano-units such as atoms, molecules, and nanomaterials [95–97]. Rather than a completely new concept, it is more of an integration of existing concepts. In other words, it is a fusion of nanotechnology with various material-related sciences and peripheral fields (organic chemistry, inorganic chemistry, coordination chemistry, polymer chemistry, supramolecular chemistry, bio-related chemistry, microfabrication technology, etc.). The following elemental technologies for building functional material systems from nano-units can be considered: atomic/molecular-level manipulation, chemical/physical material transformation including organic synthesis, self-assembly/self-organization, alignment and orientation by application of external fields and energy, nano/microfabrication, and biochemical/biotechnological processes [98]. These are selected and combined as appropriate. Compared to self-assembly, which is a single-equilibrium process, it is often a multistep process. Accordingly, nanoarchitectonics is well suited to creating asymmetric and hierarchical structures [99]. In addition, the underlying nanoscale interactions often involve uncertainties such as thermal fluctuations, stochastic distributions, and quantum effects. Therefore, the various effects are harmonized rather than simply added together [100].

The above principles are general and independent of the type of materials and their functions. Nanoarchitectonics will be universally applicable to a wide variety of material systems. Originally, all matter is composed of units of atoms and molecules. Therefore, the concept of nanoarchitectonics, which is the architecture of matter from atoms and molecules, can be the creation of all matter. Like the ultimate theory of everything in physics [101], it could become a method for everything [102,103], an integrated concept for synthesizing functional materials in materials science. In fact, many papers advocating nanoarchitectonics have been published in recent years. The field ranges from basic to applied sciences. It includes material synthesis [104–114], creation of specific structures [115–125], organization of structures [126–138], exploration of basic physical phenomena [139–150], basic biochemistry [151–163], catalysis [164–175], environmental remediation [176–187], sensors [188–197], devices [198–205], energy generation [206–214], energy storage [215–222], drug delivery [223–227], cellular control [228–231], and biomedical applications [232–242]. Since nanoarchitectonics is a comprehensive concept, there are also many approaches that do not advocate nanoarchitectonics but have the same effect as nanoarchitectonics.

However, nanoarchitectonics, which creates intricate three-dimensional functional structures, is not always easy. Two-dimensional nanoarchitectonics based on reactions and arrangements at the surface may be an easier target to tackle. A better methodology would be to define a two-dimensional structure and then develop it into a three-dimensional structure and function. It is a structure development prescription from interface to bulk. Such an approach can be seen in several existing research examples. A typical approach is the interface-based nano thin film fabrication technique. One typical approach is the Langmuir–Blodgett (LB) method [243–249]. A thin film at the monolayer level is first prepared at a two-dimensional liquid interface, such as a water surface. If these films are sequentially transferred onto a substrate, a three-dimensional, multilayered structure is formed. Layer-by-layer (LbL) assembly is a simpler and more versatile method than the LB method, although its structural control is more ambiguous [250–256]. Based on specific interactions; thin films are sequentially deposited on a substrate to obtain a variety of thin film structures. If this technique is performed on colloidal templates, it is possible to fabricate three-dimensional thin-film capsules. These techniques are widely studied as a powerful method to convert two-dimensional nanoarchitectonics into three-dimensional structures. However, the resulting structures are still at the thin-film level and may be described as somewhat thicker two-dimensional nanoarchitectonics. Other than these methods, nanoarchitectonics conversion from two dimensional to three dimensional has to be considered.

This review aims to discuss other possibilities of methodologies that expand from some two-dimensional nanoarchitectonics to three-dimensional structures and functions. Three typical examples are presented (Figure 2) that fall under this research orientation, regardless of what is advocated for nanoarchitectonics. The first is the control of bulk materials through nanoarchitectonics of two-dimensional surfaces. This is illustrated by the example of controlling the orientation of a bulk liquid crystal by changing the structure of a very thin surface layer. The second is rational structural architecture from two dimensional to three dimensional. Several examples of metal–organic frameworks (MOFs) and covalent organic frameworks (COFs) from two-dimensional control to three-dimensional architecture are given as examples for this purpose. The third category is the control of cells by surfaces. Cells originally have a cascading signal-generated growth mechanism [257–259]. Contact with a two-dimensionally nanoarchitectonized interface can induce advanced functions of the cell. This can be introduced as amplification from two-dimensional nanoarchitectonics to three-dimensional function.

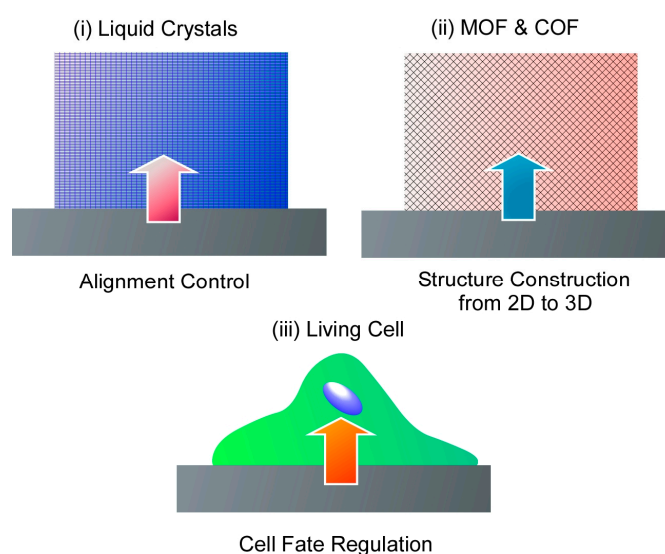


**Figure 2.** Three topics presented in this review article: (i) 2D to 3D dynamic structure control: liquid crystal commanded by the surface; (ii) 2D to 3D rational construction: MOF and COF; (iii) 2D to 3D functional amplification: cells regulated by the surface.

According to the above backgrounds, this review paper is organized as follows. This introduction is followed by a summary of the three issues introduced in the previous paragraphs. They are the following sections: (i) 2D to 3D dynamic structure control: liquid crystal commanded by the surface; (ii) 2D to 3D rational construction: MOF and COF; (iii) 2D to 3D functional amplification: cells regulated by the surface. In addition, this review summarizes the important aspects of the ultimate three-dimensional nanoarchitectonics as a perspective. The goal of this paper is to establish an integrated concept of functional material creation by reconsidering various reported cases from the viewpoint of nanoarchitectonics. Nanoarchitectonics can be regarded as a method for everything in materials science.

## 2. 2D to 3D Dynamic Structure Control: Liquid Crystal Commanded by the Surface

Liquid crystals are materials that can flexibly change their structures while maintaining a certain degree of orientation and other organizing ability [260–262]. In Ichimura's review article on the optical control of liquid crystals [263], the behavior of liquid crystals incorporating photochromic molecules is discussed. Photochromic molecules are usually embedded in various matrices in both fundamental and practical research. In such cases, the structural transformation of the photochromic guest molecule alters the reversible properties of the matrix, the liquid crystal. The orientation of the host molecules and residues that act as the matrix is changed. Broadly speaking, photoaligned liquid crystal systems fall into two types. The first type consists of liquid crystal molecules doped with photochromic units. The light-induced structure of a few photochromic chromophores results in the reorientation of the majority of matrix liquid crystal molecules. This leads to the generation of large optical anisotropy. Another type of liquid crystal system reflects the photoalignment state of photochromic molecules attached to the substrate surface into the bulk liquid crystal layer. This type of structural change in the surface, in which minute structural changes on the surface dictate structural changes in many of the molecular layers above it, is called a command surface [264,265]. This technique demonstrates the effective application of photochromic units to fabricate liquid crystal photoresponsive systems. It also opens the way to the control of photoalignment of liquid crystals, even with irreversible photochemistry. This concept is not only performed by photochromic molecules. It can be a methodology to expand broadly two-dimensional nanoarchitectonics to three-dimensional liquid crystal functionality. It can also be an effective method for fabricating new types of optical elements and devices for photonics applications.

One of the pioneering examples of the command surface concept can be found in the report of Seki, Ichimura, and co-workers [266]. In this study, LB films of side-chain azobenzene amphiphilic polymers were used as photochromic command layers. The photoisomerization of the command layer was used to control the reversible homeotropic planar photochemical orientation of nematic liquid crystals. As a nanoarchitectonics strategy for the command surface, it is important that the azobenzene photochromic unit is separated from the background, the poly(vinyl alcohol) backbone, by a methylene spacer of appropriate length. With this molecular design, a single azobenzene monolayer is sufficient to induce a change in thick liquid crystal orientation. For LB nanoarchitectonics, the vertical transfer method of preparation is more advantageous. The vertical transfer method produced more homogeneously aligned LB films and the liquid crystal molecules were oriented parallel to the immersion direction. When linearly polarized UV light was irradiated, the liquid crystalline molecules reoriented in the direction perpendicular to the polarization plane. In other words, the trans–cis isomerization of the highly photoreactive azobenzene photochromic units in the polymer LB layer successfully commanded the orientation between the homeotropic and planar modes of the nematic liquid crystal.

The orientation of liquid crystal molecules is largely governed by the degree of freedom of the surfaces with which they come into contact and other factors. As in the above example, the photoresponsive layer on the surface with freedom serves as the command layer of the side-chain liquid crystal polymer film. Various studies have been conducted

to understand the interfacial behavior of these liquid crystal molecules. For example, the photoalignment behavior of nematic liquid crystals on azobenzene polymer films has been the subject of research. Hara, Seki, and co-workers have investigated the optical orientation behavior of side-chain liquid crystalline azobenzene polymer films with a thickness of approximately 400 nm and a 35  $\mu\text{m}$ -thick low-molecular-weight nematic liquid crystal, 4'-pentyl-4-cyanobiphenyl in situ at the interface (Figure 3) [267]. In addition to polarized light optical microscopy observations, small-angle X-ray scattering measurements were used to evaluate the structure inside the liquid crystal-injected sandwich cell. This technique has provided new insights into the behavior of liquid crystal molecules in the vicinity of alignment films on solid substrates. For example, they have succeeded in detecting the selective and time-series structuring and orientation of mesogens at the interface in the formation of smectic layers. A highly ordered smectic liquid crystalline phase is induced by the hybridization of the mesogens of azobenzene polymers and 4'-pentyl-4-cyanobiphenyls. A cooperative hybrid highly ordered smectic liquid crystal phase is formed by weak electron transfer at interfacial contact. Such analysis is important to understand how slight structural changes at the two-dimensional interface are reflected in the three-dimensional structure. Direct X-ray observations in intact liquid crystal cell systems provide useful information on the driving mechanism. It can be a powerful tool in industrial applications in terms of liquid crystal device design. It should also expand the possibilities in terms of practical applications.

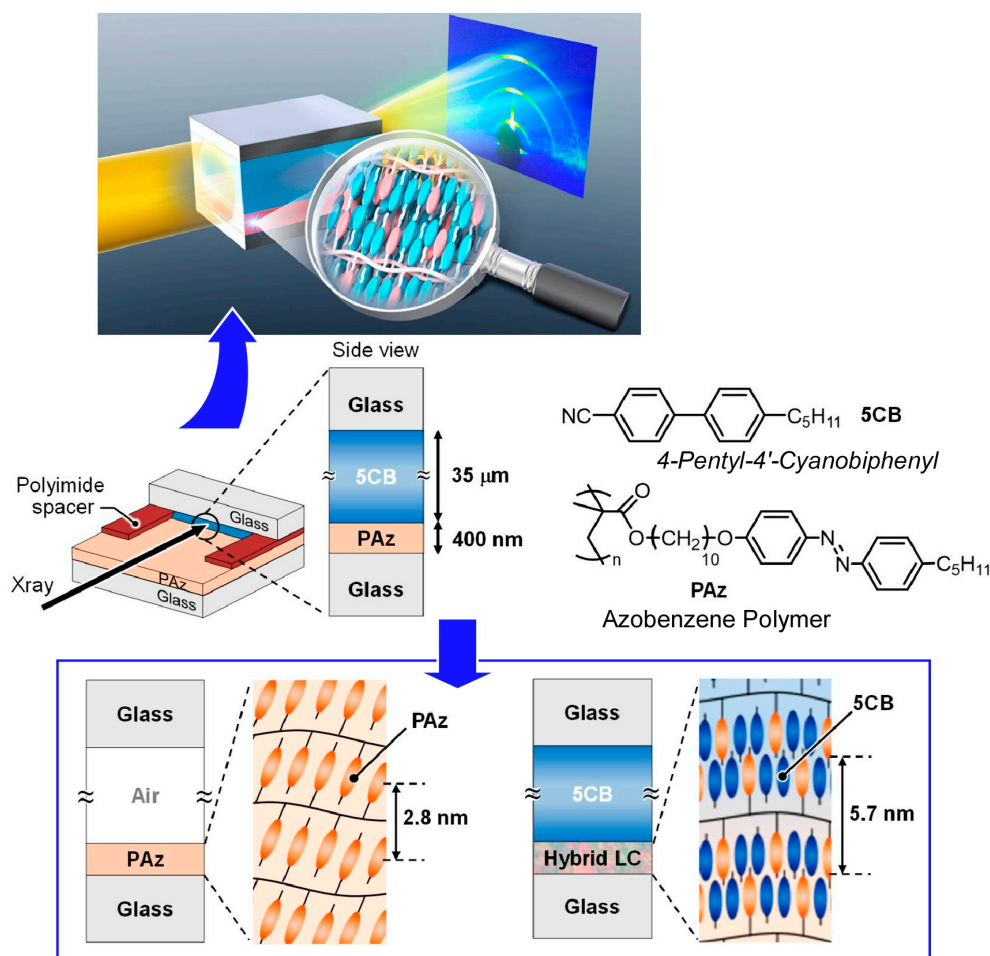


**Figure 3.** Evaluation of the optical orientation behavior of side-chain liquid crystalline azobenzene polymer films with a thickness of approximately 400 nm and a 35  $\mu\text{m}$  thick low-molecular-weight nematic liquid crystal, 4'-pentyl-4-cyanobiphenyl in situ at the interface. Reprinted with permission from [267]. Copyright 2023 American Chemical Society.

Lundin and co-workers used electrospinning to fabricate core–sheath nanofibers with photochromic and liquid crystalline components (Figure 4) [268]. The core–sheath nanofibers consist of a polyvinylpyrrolidone sheath doped with a photochromic azobenzene surfactant and a low-molecular-weight nematic liquid crystal core. By incorporating the azobenzene surfactant into the polymer sheath, the nematic-to-isotropic transition temperature of the liquid crystal core could be photochemically controlled. In other words, ultraviolet (UV) irradiation reduced the phase transition temperature. At high surfactant content, the temperature of the photo-induced phase transition was reduced to below room temperature. It allows “turning on” and “turning off” the birefringence of the nanofibers upon UV irradiation and does not require external heating. Photoisomerization of azobenzene surfactants at the poly(vinylpyrrolidone)/liquid crystal interface causes surface-induced disordering of the liquid crystal core. Therefore, UV irradiation causes a change from planar-axis orientation to random orientation. In the case of visible light irradiation, the opposite change is expected to occur. Thus, the photochromic nature of this core–sheath nanofiber system is the result of the difference in the compatibility of the *cis*- and *trans*-isomers with the liquid crystal matrix at the liquid crystal/polymer interface. Similar to the command surface of LB films described above, the incorporation of azobenzene into the polymer sheath of liquid-crystalline-core nanofibers allows molecular changes to be reflected in the three-dimensional properties of the liquid crystal.

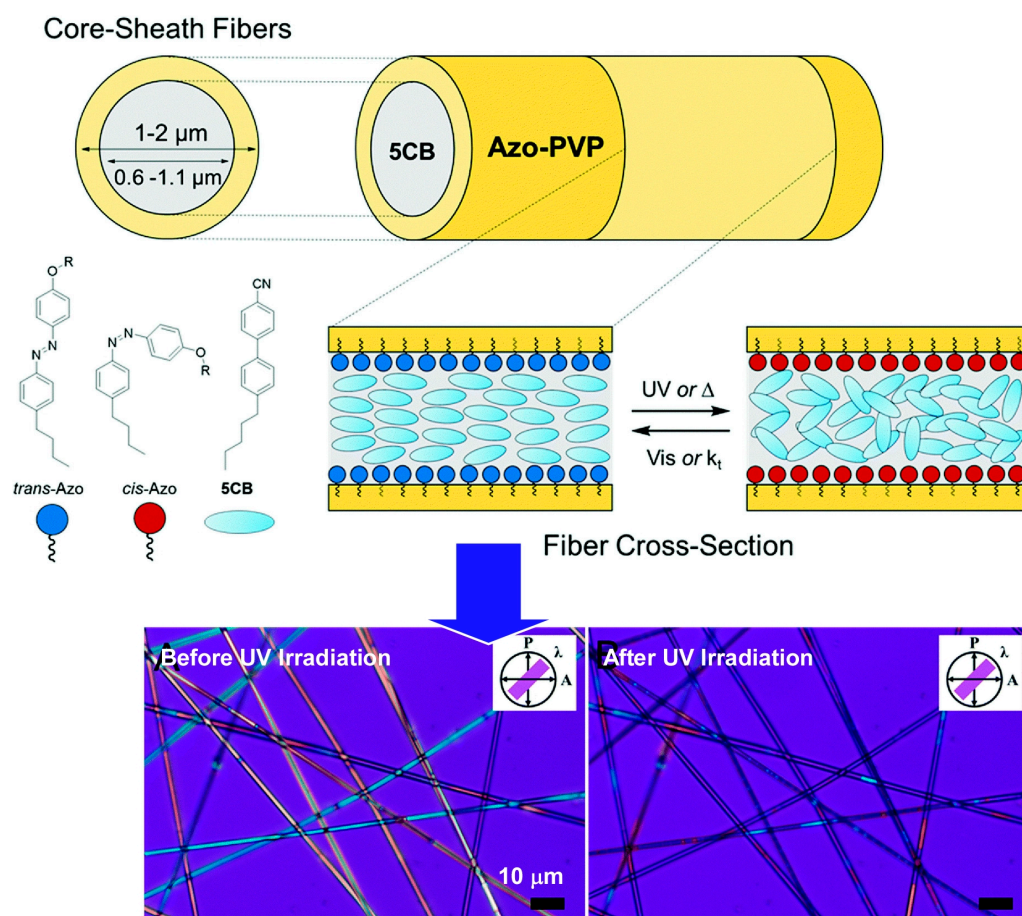


**Figure 4.** Nematic-to-isotropic transition of liquid crystalline components doped with a photochromic azobenzene surfactant in core–sheath nanofibers. Reprinted with permission from [268]. Copyright 2021 Royal Society of Chemistry.

The optical control of liquid crystal molecules as an example of how two-dimensional nanoarchitectonics through molecular design and orientation is reflected in the properties of three-dimensional materials. Not only LB-type monolayers, but also polymer layers

with a core-shell structure act as a command surface. The molecular-level phenomena of structural and orientation changes on the command surface are amplified into three-dimensional material properties such as liquid crystal orientation and phase transitions. The key to this process is molecular phenomena at the interface. The control of the interface leads to the amplification of functional structures from two to three dimensions.

### 3. 2D to 3D Rational Construction: MOF and COF

The synthetic approaches of metal–organic frameworks (MOFs) [269–279] and covalent organic frameworks (COFs) [280–284] are methods for rationally building structures from molecular units and ions. These structures are often formed as two-dimensional structures in interfacial environments, although they can also be obtained in three-dimensional structures such as crystals. As a rational nanoarchitectonics from two dimensions to three dimensions, material designs based on MOFs and COFs are beneficial. In this section, several approaches to three-dimensional architecting from two-dimensional MOFs and COFs are exemplified.

Structural evolution from two dimensions to three dimensions is a useful technique for tuning mechanical properties. For example, developing strategies to improve the structural robustness of COFs has been recognized as very important. Yu, Zhang and co-workers reported a method to rationally design and synthesize crosslinked COFs in which the two-dimensional COF layers are covalently fixed and linked by poly(ethylene glycol) (PEG) three-dimensional or alkyl chains (Figure 5) [285]. It is a bottom-up synthetic strategy to structuralize layered structures of two-dimensional COFs using monomers linked by flexible PEG or alkyl chains. The two-dimensional layered structure was converted into a quasi- three-dimensional accumulation framework via covalent crosslinking, where vertical crosslayer bonding is dominant. All synthesized crosslinked COFs were highly crystalline and porous. In particular, they exhibited robust structural stability that surpassed that of typical two-dimensional COFs. While simple assemblies of two-dimensional COFs were easily exfoliated into nanosheets by sonication, pulverization, and water treatment, three-dimensional crosslinked COFs maintained their ordered framework even after such treatments due to the crosslinking effect. The structural stability while inheriting high crystallinity and porosity provides the interlayer stability that is extremely necessary for advanced applications such as heterogeneous catalytic reactions and proton/ion transport. A high application potential of quasi-three-dimensional COFs is expected.

Three-dimensional COFs are of interest as a structurally stable group of materials with their inherent large number of open sites and pore confinement effects. However, it is not easy to generate an entangled three-dimensional network formed from multiple two-dimensional layers inclined toward each other. Ma, Li, and co-workers have successfully synthesized a new three-dimensional COF based on a two-dimensional network with interpenetrations (Figure 6) [286]. The structures were formed by [3+2]imine condensation reactions using triangular knots and linear linkers. Specifically, they were formed by [3+2]imine condensation reactions using 1,3,5-triformylbenzene and 2,3,5,6-tetramethyl-1,4-phenylenediamine. The range of strategies for achieving three-dimensional COFs was broadened by mutual coordination. Such examples demonstrate that structurally complex extended frameworks can be obtained from simple molecules and can be used for nanoarchitectonics. They enrich synthetic strategies for three-dimensional COFs and greatly expand the range of COF materials.

Gui, Sun, and Wang and co-workers devised a method to form three-dimensional COFs by introducing steric hindrance to molecular blocks that inhibit  $\pi$ – $\pi$  stacking, as a method for two-dimensional COFs to intertwine with each other (Figure 7) [287]. In this approach, highly crystalline COFs are synthesized starting from rationally designed precursors containing longitudinally bulky anthracene units. Structurally, the presence of anthracene groups outside the  $C_{2h}$  symmetry plane strongly inhibits  $\pi$ – $\pi$  interactions. As a result, the formation of square entanglement is promoted. Furthermore, the fluorescence synthesized here can be used as a sensor to detect trace amounts of antibiotics in water. It

is promising to construct three-dimensional COFs by entanglement of two-dimensional layers from precursors with bulky groups in the vertical direction of the skeleton shown in this example. This strategy would open the door for the design and synthesis of many entangled COFs.

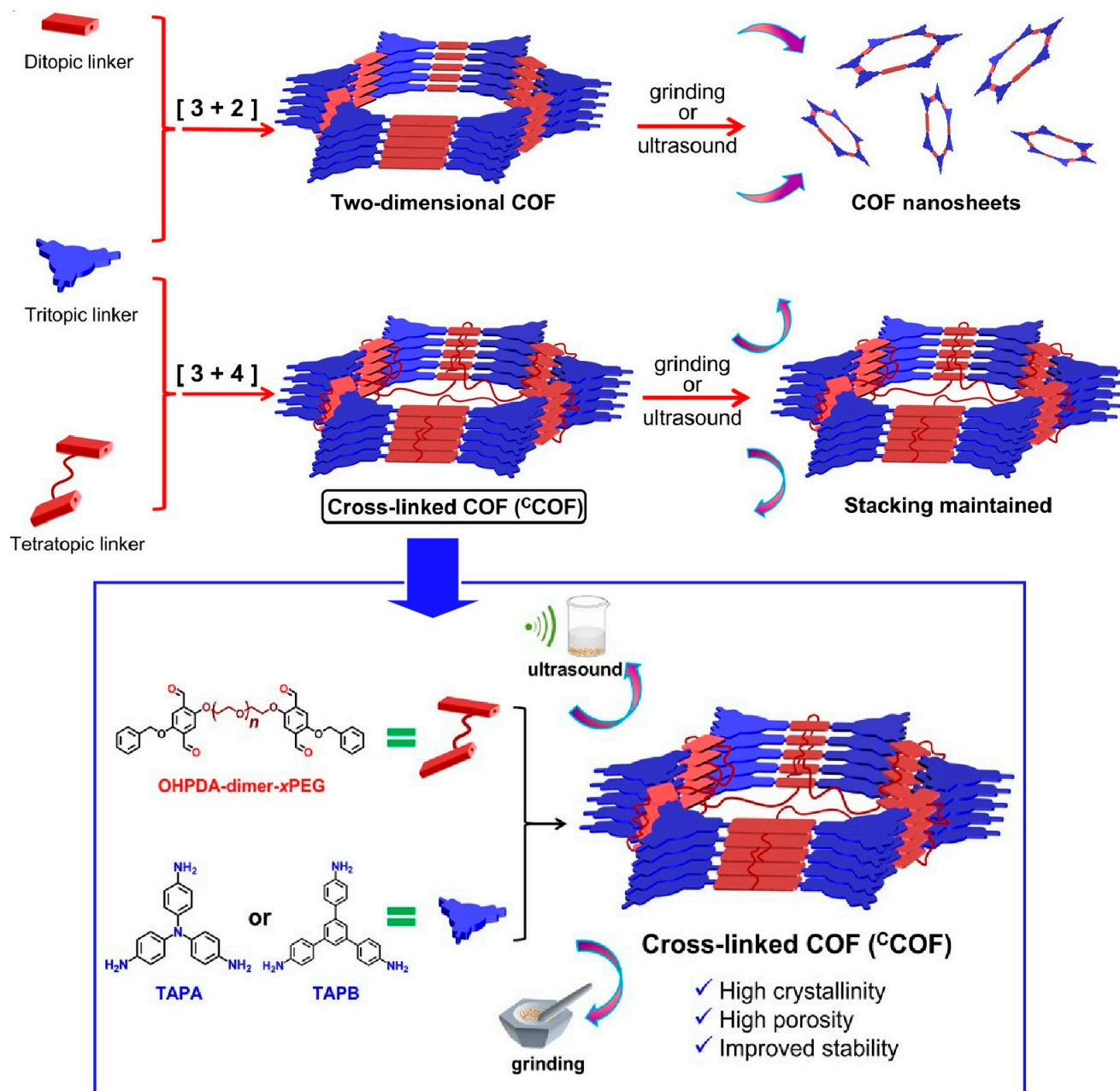


**Figure 5.** A method to rationally design and synthesize crosslinked COFs in which the two-dimensional COF layers are covalently fixed and linked by poly(ethylene glycol) (PEG) three-dimensional or alkyl chains. Reprinted with permission from [285]. Copyright 2023 American Chemical Society.

COFs can selectively interact with biomolecules due to their large surface area and well-defined pores. Their properties lend themselves to highly sensitive and selective sensing methods. Pseudo-three-dimensional COF nanosheets have shown applications in virus detection, etc. Parvin et al. synthesized pseudo-three-dimensional COF nanosheets by  $[2+2]$  imine condensation reaction between building blocks of *p*-phenylenediamine and 2,5-furandicarbaldehyde [288]. Then, trend-based detection of biomolecules, in-

cluding COVID-19 virus, was demonstrated (Figure 8). During the synthesis process, a two-dimensional sheet was initially formed, which was later converted into a stable pseudo-three-dimensional structure by changing the bond angles. Furthermore, exfoliation techniques were used to produce nanosheets with reduced  $\pi$  stacking. The exfoliation of COFs into nanosheets provides highly porous structures. The pseudo-three-dimensional COF nanosheet created in this research functions as an adsorbent for biomolecular probes. In addition, it also functions as an acceptor to quench the fluorescence of Texas Red dye-labeled probes. This enabled sensitive and selective fluorescence-based detection of biomolecules, including COVID-19 virus, with a low detection limit of 2 picomoles. Pseudo-three-dimensional COF nanosheets exhibited advantages over conventional graphene oxide, including large surface area, pore structure, specific channel structure, multidimensionality, and stability. Since no catalyst is used in the synthesis process, simpler and more cost-effective production methods can be employed. It also does not require complex and time-consuming procedures such as RT-PCR. These materials have potential applications in the detection of various diseases, electronic devices, and membrane separations.

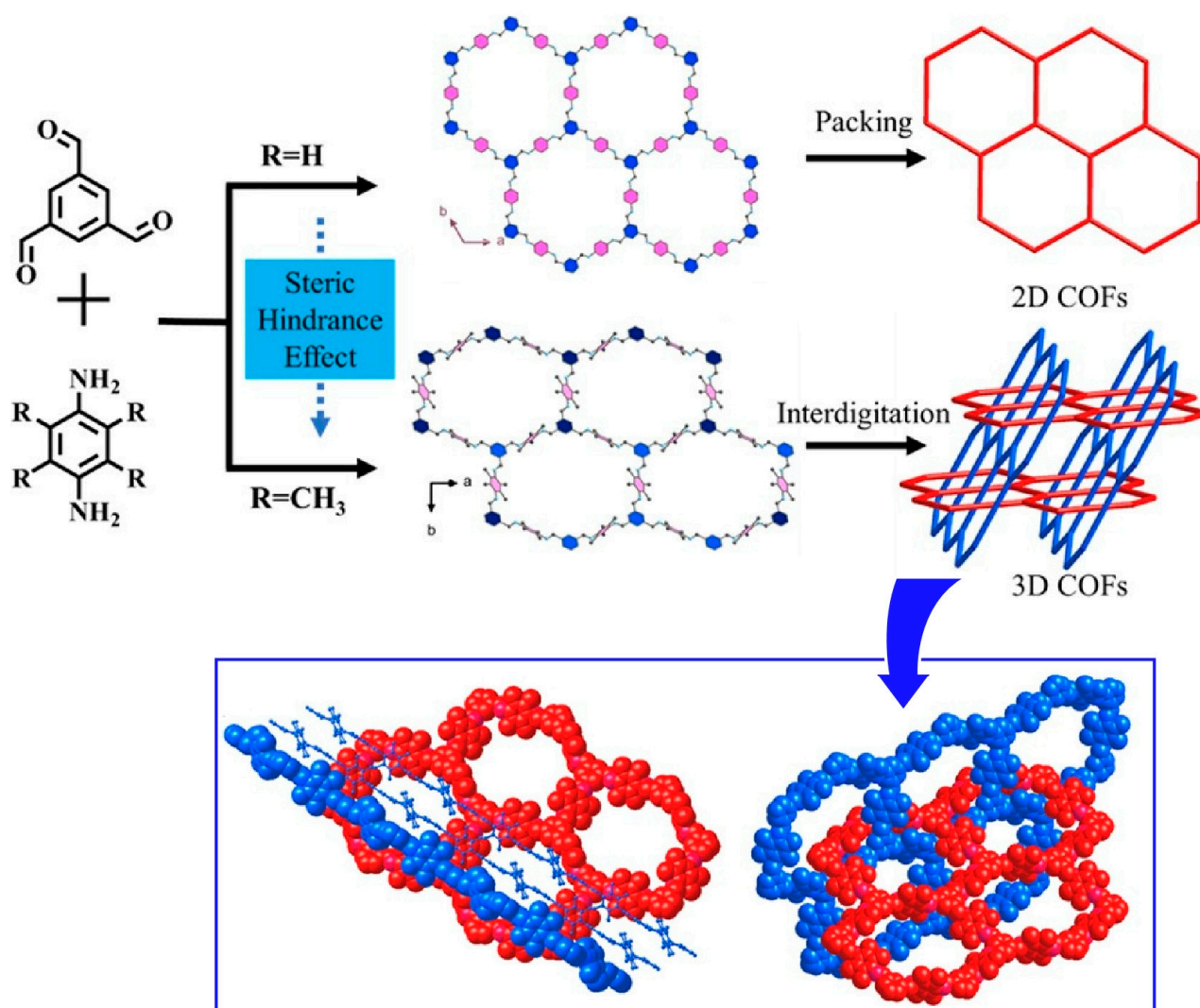


**Figure 6.** Nanoarchitectonics of three-dimensional COFs based on a two-dimensional network with interpenetrations where the structures were formed by [3+2]imine condensation reactions using triangular knots and linear linkers. Reprinted with permission from [286]. Copyright 2023 American Chemical Society.

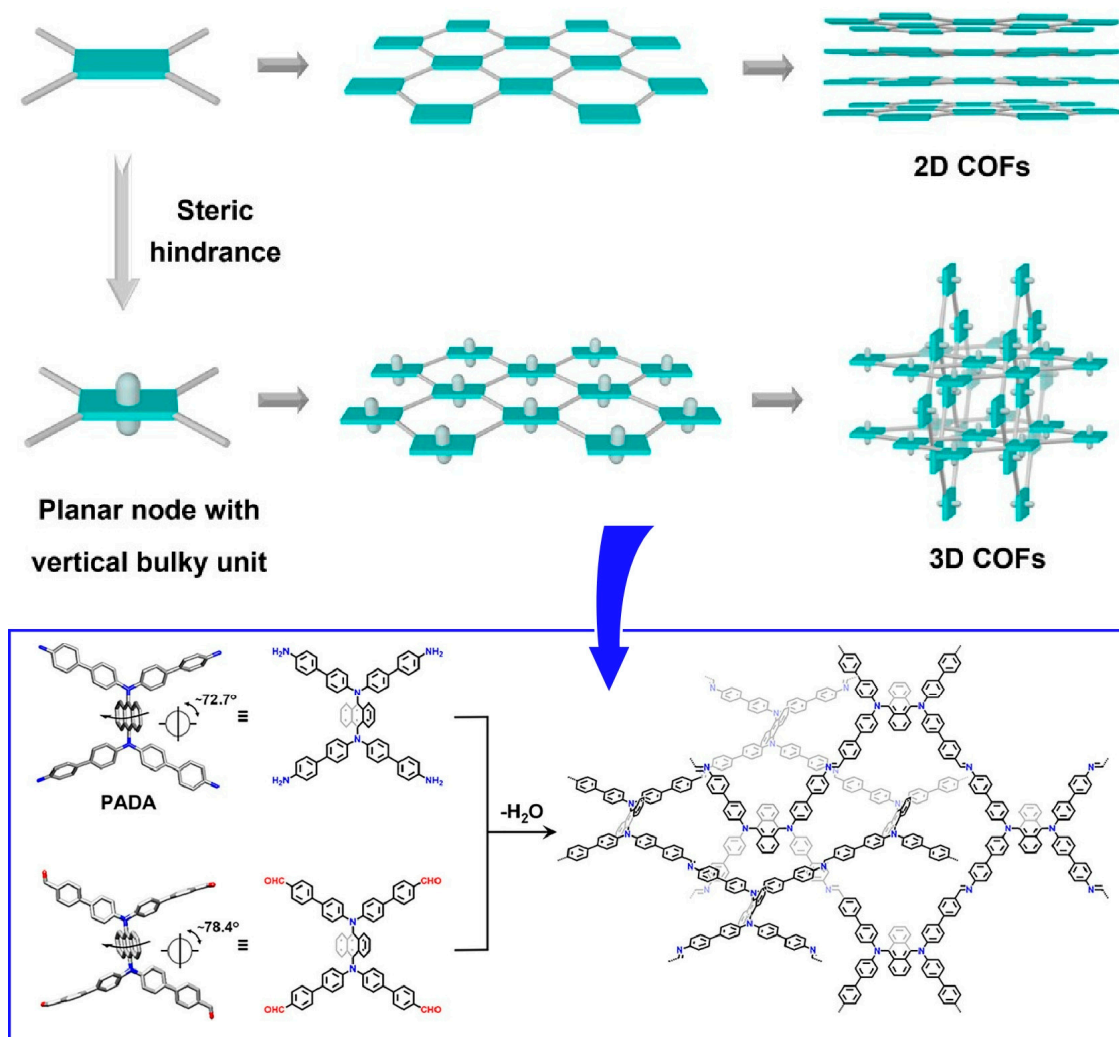


**Figure 7.** A method to form three-dimensional COFs by introducing steric hindrance to molecular blocks that inhibit  $\pi$ - $\pi$  stacking, as a method for two-dimensional COFs to intertwine with each other. Reprinted with permission from [287]. Copyright 2023 American Chemical Society.

Oña-Burgos and co-workers have developed a stable structure consisting of two pairs of two-dimensional nanosheets [289]. In other words, they synthesized a new cobalt MOF based on a well-defined layered double core strongly bound by intermolecular bonds (Figure 9). Its three-dimensional structure is maintained by  $\pi$ - $\pi$  stacking interactions between the unstable pyridine ligands of the nanosheets. In an aqueous solution, the axial pyridine ligands are exchanged with water molecules. This results in the exfoliation of the material. In such cases, the individual double nanosheets maintain their structures. Furthermore, the original three-dimensional layered structure is restored by a solvothermal process using pyridine. During the exfoliation-columnarization process, the material exhibits a memory effect. This two-dimensional MOF also exhibits electrocatalytic activity. Electrochemical activation of the two-dimensional cobalt MOF  $\cong$  nafion-modified electrode improves both ion and electron transfer across the membrane. The formation of electrocatalytically active cobalt centers is then promoted. The activated composite exhibited enhanced electrocatalytic activity for the oxidation of water in neutral media. Spectroscopic and electrochemical characterizations were performed. The nanosheets have a special topology in which the cobalt centers are quite far apart. A mononuclear center-dependent reaction pathway mechanism has been proposed for the cobalt-mediated electrocatalytic oxygen evolution reaction. This electrocatalyst has a better TOF value and robustness than reported for similar electrocatalysts.

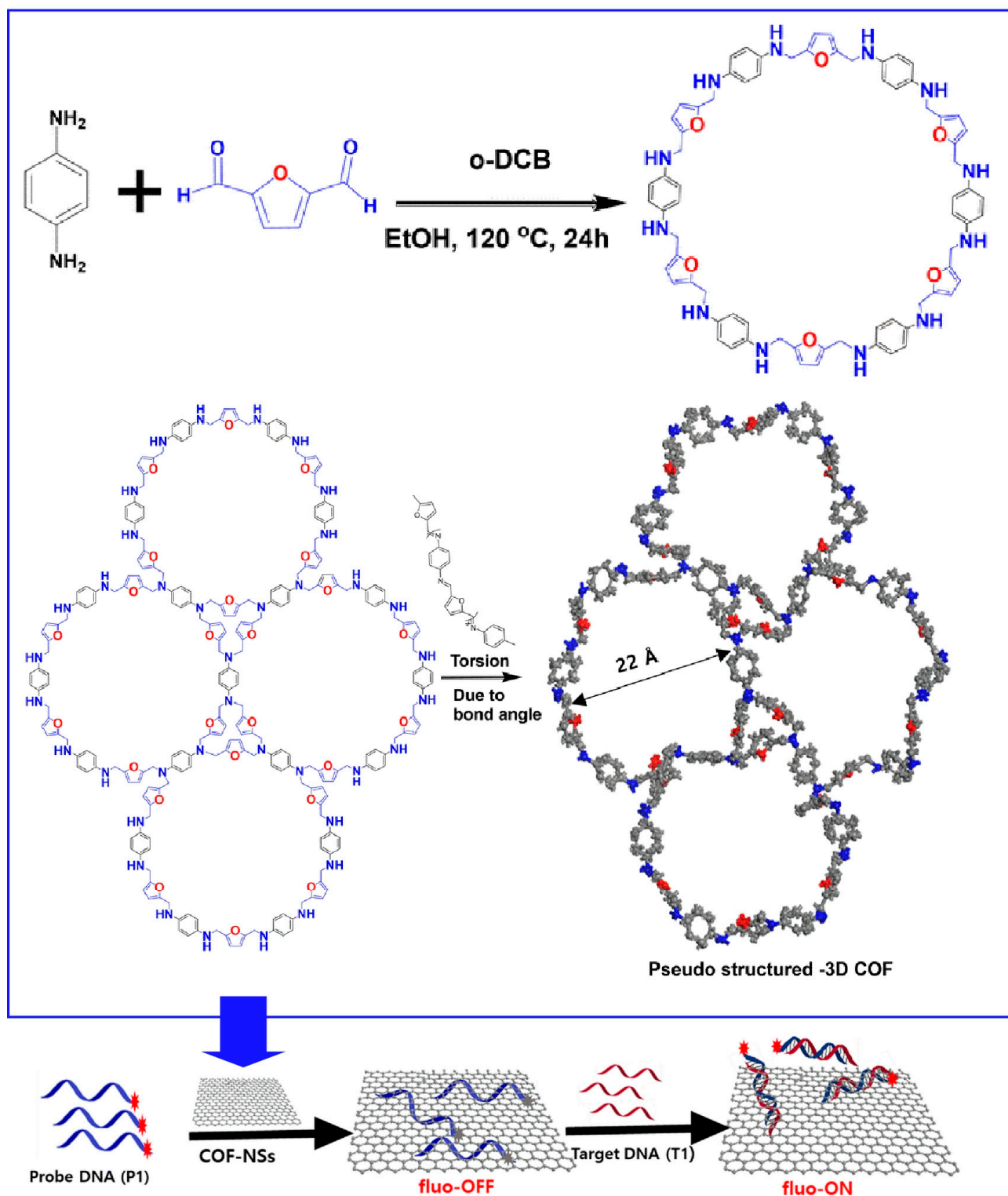


**Figure 8.** Pseudo-three-dimensional COF nanosheets for detection of biomolecules, including COVID-19 virus where the pseudo-three-dimensional COF nanosheet functions as an adsorbent for biomolecular probes and an acceptor to quench the fluorescence of dye-labeled probes. Reprinted with permission from [288]. Copyright 2023 Royal Society of Chemistry.

The construction of two-dimensional nanosheets into three-dimensional ordered structures facilitates mass transfer. The full potential of two-dimensional building blocks can be exploited in applications such as catalytic reactions. Zou et al. reported the synthesis

of organometallic frameworks with orthogonal nanosheet arrays (Figure 10) [290]. Cubic MOFs are used as the core, and single-crystalline MOF nanosheets with naturally occurring non-preferred faceted exposures are epitaxially grown on top of them as shells. The nanoarchitectonized nanosheets have two typical shapes and crystallographic orientations. Nevertheless, they form an orthogonally aligned single-crystal framework. It is possible to obtain MOFs with a single composition and hollow orthogonally aligned nanosheet morphology. It has the characteristics of peculiar facet exposure and macroporous structure. Therefore, the electrocatalytic oxygen evolution activity is improved compared to conventional nanosheets. This structure exposes unsaturated active sites, stabilizes hydrogen-containing intermediate species, and promotes the oxygen evolution reaction process. The orthogonal arrangement of the nanosheets reduces the possibility of nanosheet re-stacking. Abundant surface active sites are provided, enhancing catalytic activity. Vertical and through pore channels are formed, facilitating diffusion of electrolyte and oxygen molecules. The hollow structure facilitates effective utilization of active sites and mass transfer, improving electrocatalytic properties. Thus, it is expected that rational function-oriented three-dimensional nanoarchitectonics strategies will lead to the design of highly functional heterostructures based on MOF nanosheets.

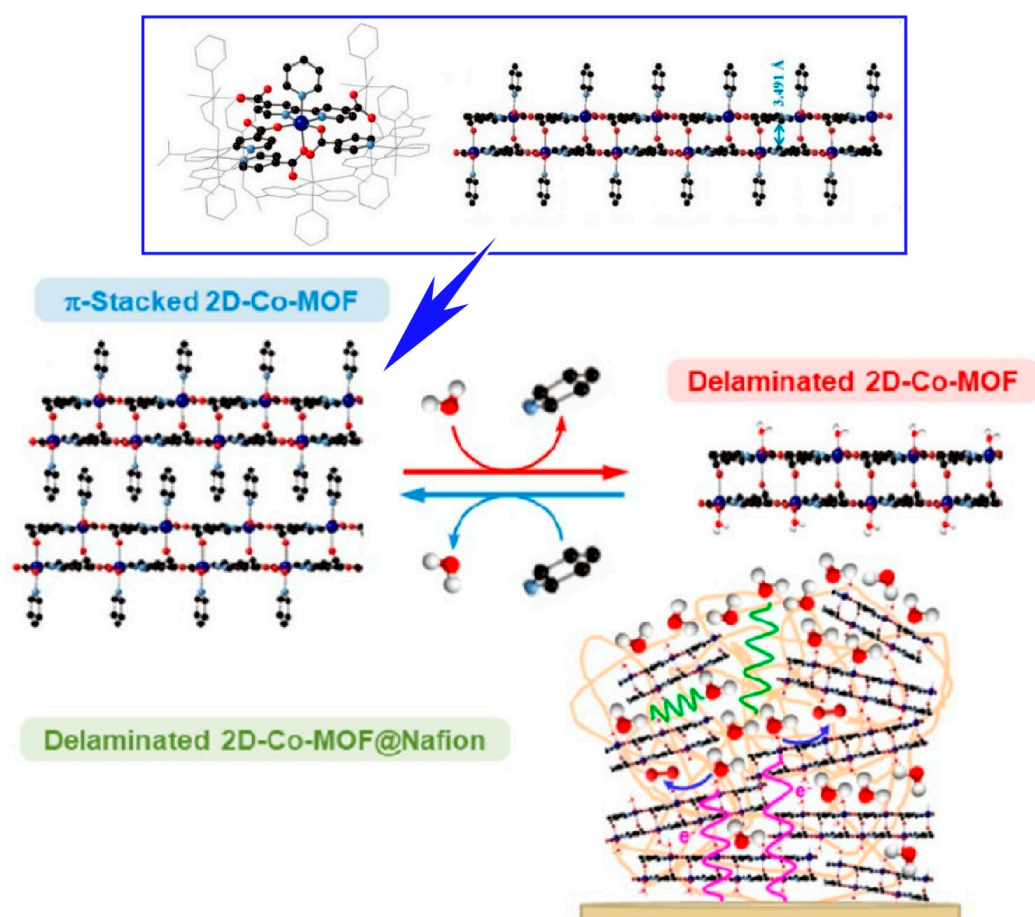


**Figure 9.** A cobalt MOF based on a well-defined layered double core strongly bound by intermolecular bonds in which its three-dimensional structure is maintained by  $\pi$ - $\pi$  stacking interactions between the unstable pyridine ligands of the nanosheets. Reprinted with permission from [289]. Copyright 2020 American Chemical Society.

The controllable fabrication of angstrom-sized channels has long been desired in fundamental studies of ion transport. This is also necessary to mimic biological ion channels. Jiang, Zhang, and co-workers reported a strategy to grow MOFs into nanochannels with angstrom-scale ion channels with one- to three-dimensional pore structures (Figure 11) [291].

One-dimensional structures with flexible pore sizes can facilitate cation transport in conductivity and mobility one to two orders of magnitude higher than MOF channels with hybrid pore shapes and sizes. Theoretical simulations and calculations show that the energy barrier for ion transport through pure one-dimensional channels is lower than through complex channel connections. The three-dimensional MOF channel also exhibited better ion sieving properties than the one-dimensional and two-dimensional MOF channels. Further studies assuming angstrom porous MOFs with various channel configurations as the building blocks will open the way to fabricate artificial ion channels of 1 nm or smaller. Applications to high-efficiency ion separation and energy conversion technologies are expected. It will also provide guidance for the development of ion separation and nanofluidics.

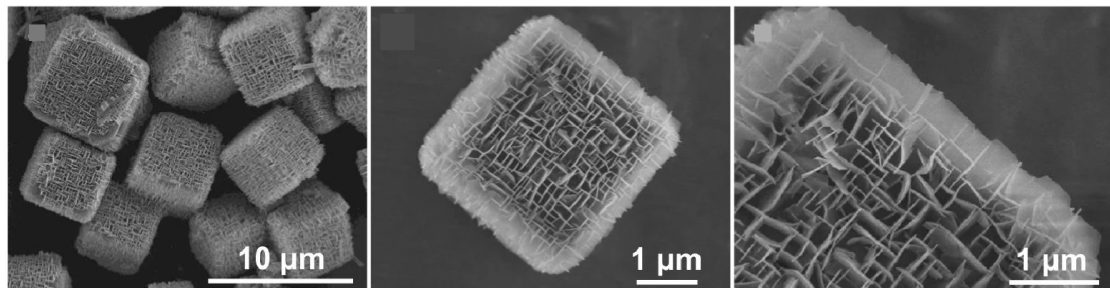


**Figure 10.** Organometallic frameworks with orthogonal nanosheet arrays for cubic MOFs. Reproduced under terms of the CC-BY license [290]. Copyright 2023 Springer-Nature.

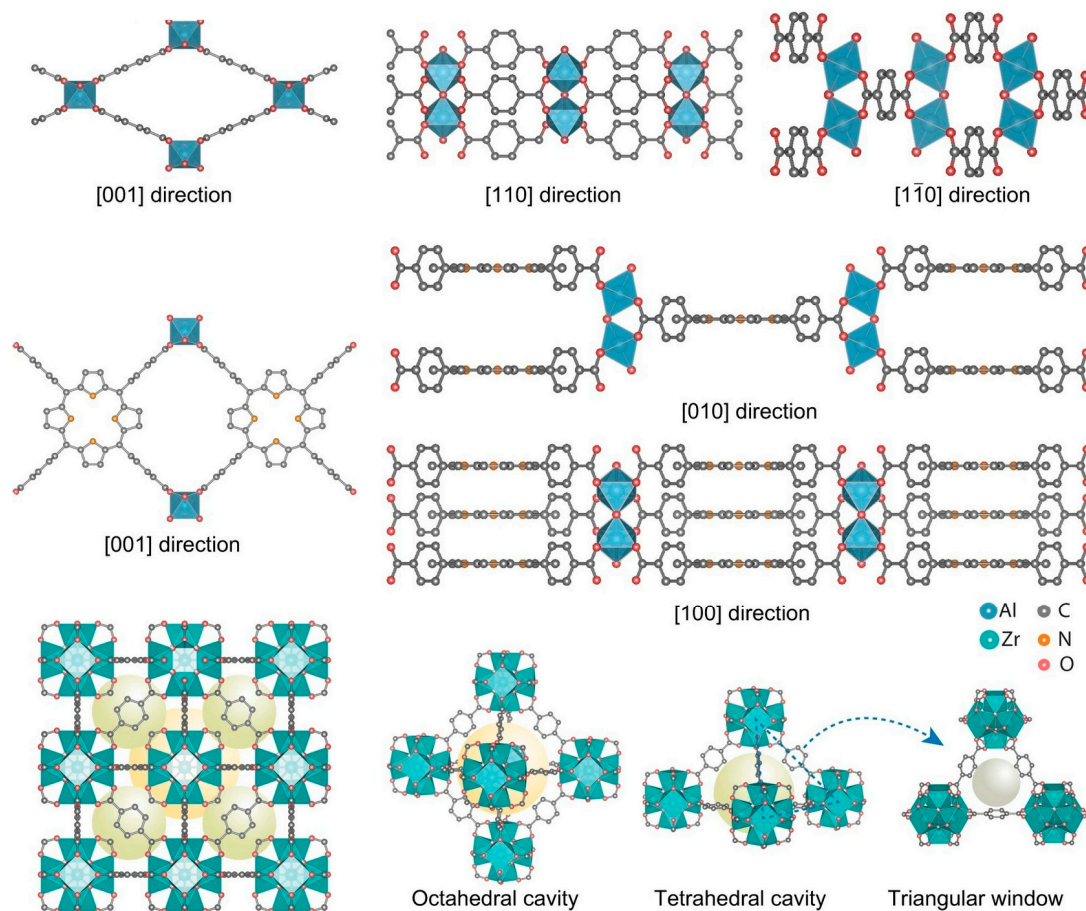


**Figure 11.** A strategy to grow MOFs into nanochannels with angstrom-scale ion channels with one- to three-dimensional pore structures. Reproduced under terms of the CC-BY license [291]. Copyright 2023 Springer-Nature.

Two-dimensional conductive MOFs have attracted much attention for their usefulness in applications ranging from electrochemical energy storage to electronic devices. However, the stacked two-dimensional structure limits access to the internal pores. The full potential has not yet been realized. Park and co-workers reported a method for converting two-dimensionally conjugated MOFs into a three-dimensional framework by post-synthetic pillar ligand insertion (Figure 12) [292]. Such structural transformation improves ion accessibility to the internal pores. As a result, there can be up to a 2-fold increase in capacitance per weight. It is expected that such nanoarchitectonics methods can be used to functionalize a variety of two-dimensional conductive MOFs. Increased accessibility through the introduction of pillars increases the potential for sensing, electronics, and energy-related applications. The pillar portion can also be given a role other than that of a spacer. For example, providing a coordination site for the pillar ligand could lead to advanced applications including electrocatalysis and sensing. The restitution of conductive MOFs from two dimensional to three dimensional and the introduction of additional functionality is expected to facilitate the volatilization of possible materials in this new field.

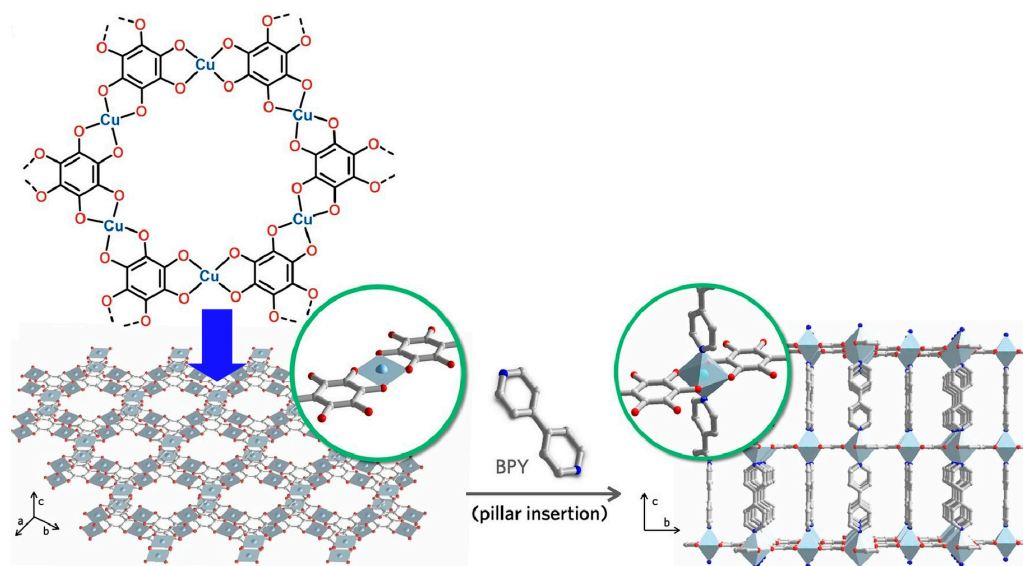


**Figure 12.** A method for converting two-dimensionally conjugated MOFs into a three-dimensional framework by post-synthetic pillar ligand insertion. Reprinted with permission from [292]. Copyright 2022 American Chemical Society.

Wee et al. reported the preparation of a new hierarchical MOF with Cu(II) centers linked by benzene tricarboxylates (BTC) (Figure 13) [293]. It is prepared by thermally induced solid-state transformation of a dense CuBTC precursor phase. It is found that ribbon-like one-dimensional constituent units transform into two-dimensional layers and finally into a three-dimensional network. The formed phases contain excess copper. The charge is compensated by hydroxyl groups, forming an open microporous framework with microporosity. This structure is useful for molecular separation. For example, it was superior to other hierarchical materials in the separation of 11-component mixtures of C<sub>1</sub>–C<sub>6</sub> alkanes. Microscopic insights into structural host–guest interactions were obtained, confirming a significant entropic contribution to molecular separation.

Li and co-workers reported the synthesis of a two-dimension-on-three-dimension (2D-on-3D) hetero-MOF structure (Figure 14) [294]. They introduced a kinetic control method using polyvinylpyrrolidone to realize an anti-epitaxial growth pattern of foreign MOF nuclei on the (111) plane of the UiO-66-NH<sub>2</sub> octahedron. This nanoarchitectonics methodology has led to the successful fabrication of 2D-on-3D MOFs with various heterostructures (Cu, Zn, Cd, Co, Ni). 2D-on-3D MOFs exhibit unique dimensional hybridization effects in the photocatalytic hydrogen evolution process in a photocatalytic hydrogen evolution

process. The photoactivity was significantly enhanced compared to the usual dimensionally identical two-dimensional, three-dimensional, and 3D-on-3D MOF structures. This can be attributed to faster electron transfer rates and more efficient electron–hole separation.

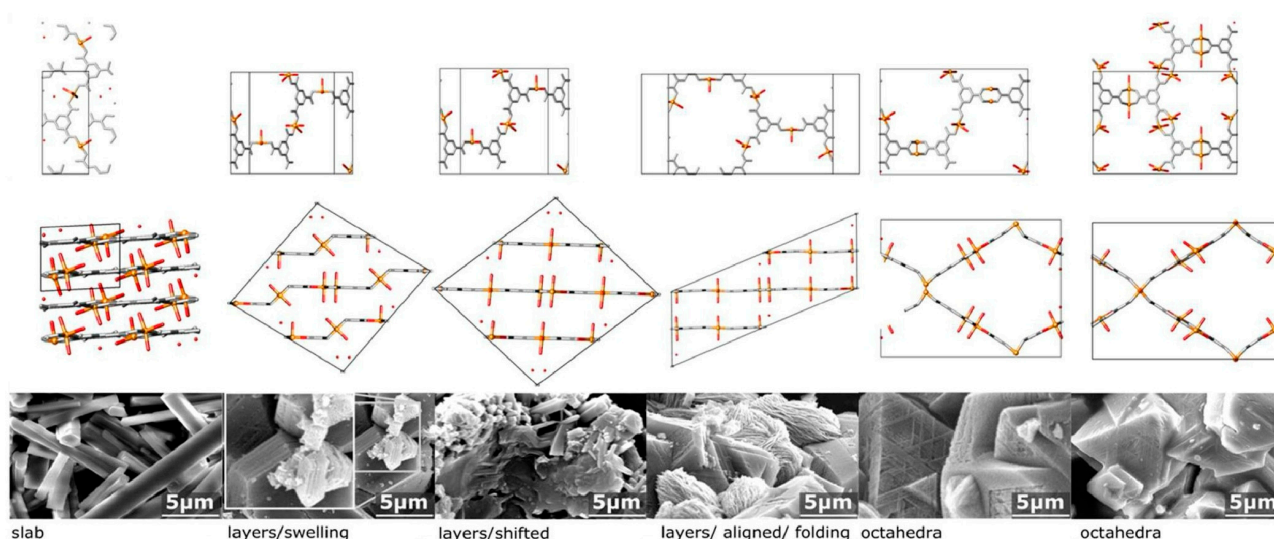


**Figure 13.** Preparation of a new hierarchical MOF with Cu(II) centers linked by benzene tricarboxylates. Reprinted with permission from [293]. Copyright 2017 American Chemical Society.

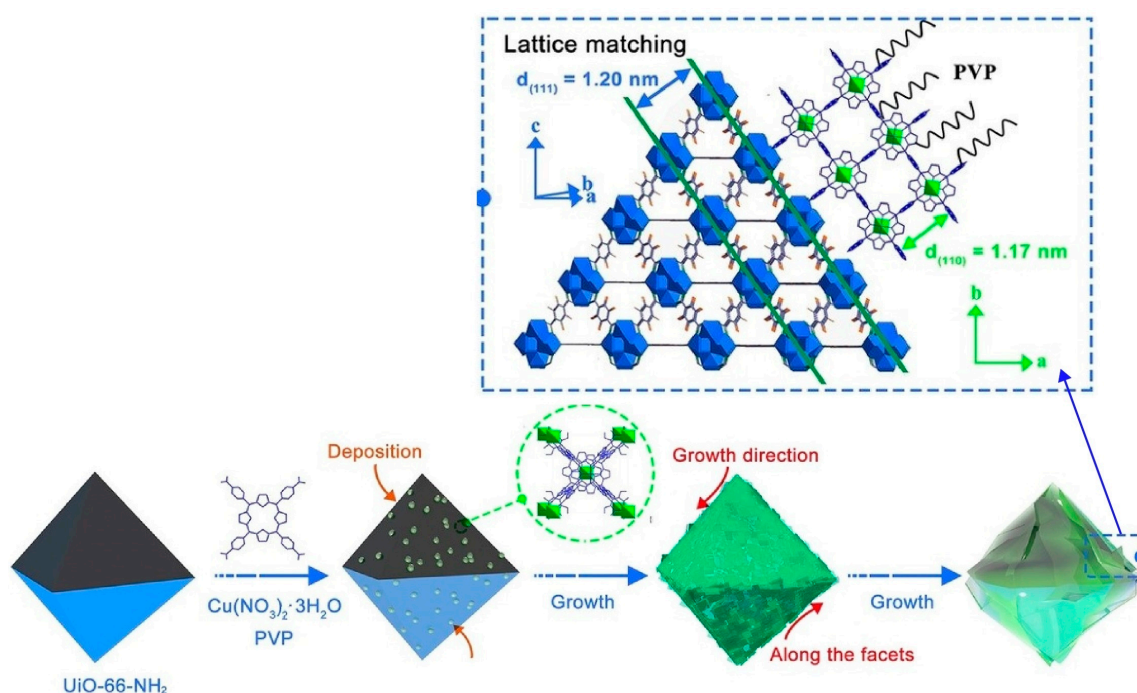


**Figure 14.** Synthesis of a two-dimension-on-three-dimension (2D-on-3D) hetero-MOF structure. Reprinted with permission from [294]. Copyright 2022 Wiley VCH.

Conversely, there are examples where dimensional reduction nanoarchitectonics of MOF structures from three dimensions to two dimensions is functionally superior. For example, a dimensional reduction approach has been proposed to improve the cryopreservation efficiency of red blood cells by MOFs. Such an approach takes the methodology of a stepwise reduction in three-dimensional MOF nanoparticles into two-dimensional ultrathin metal–organic layers (MOLs). Guo, Zhu, and co-workers synthesized a series of hafnium (Hf)-based two-dimensional metal–organic layers with different thicknesses (from single

layer to stacked multilayers) and densities of hydrogen-bonding sites (Figure 15) [295]. Two-dimensional MOLs enhance the interaction of interfacial hydrogen-bonded water networks due to their high surface-to-volume ratio. This increases the utilization of internally ordered structures. The ability of the hydrogen donor group to recognize and match ice crystal planes can effectively inhibit ice growth and recrystallization for red blood cell cryopreservation. Thin-layered Hf-MOL was found to have significantly better ice recrystallization inhibitory activity and superior cell retrieval efficiency compared to three-dimensional MOL. Flexible two-dimensional MOLs have a higher density of hydrogen donor groups compared to three-dimensional MOF nanoparticles, which have a rigid structure and limited exposure of lattice planes. They also have smaller steric hindrance. These structural advantages may account for the marked efficiency of MOFs in ice suppression and erythrocyte recovery.

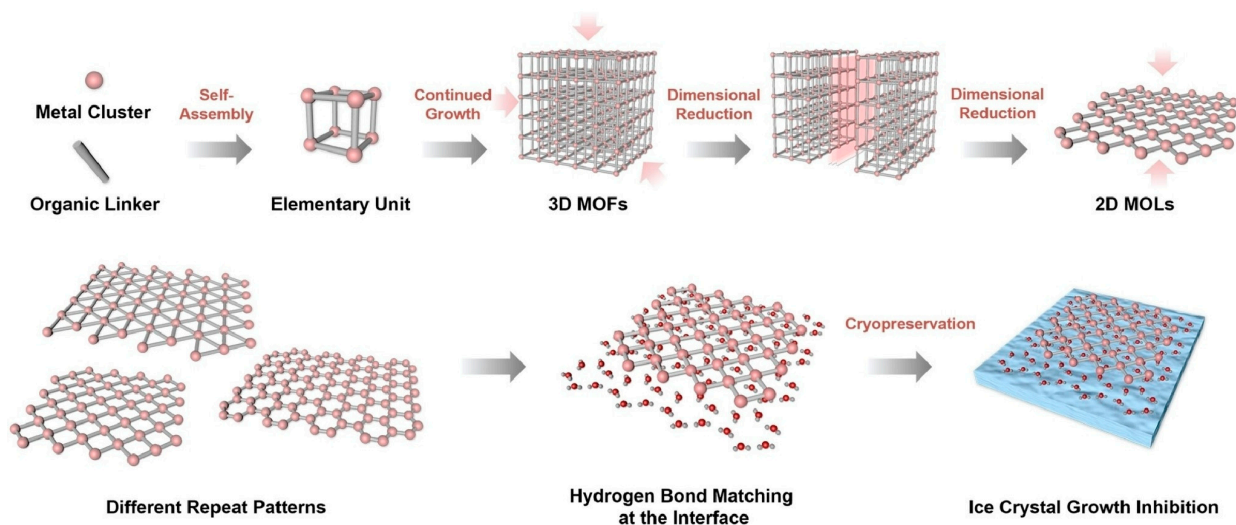


**Figure 15.** Synthesis of a series of hafnium (Hf)-based two-dimensional metal–organic layers with different thicknesses (from single layer to stacked multilayers) and densities of hydrogen-bonding sites with inhibition capability of ice growth. Reprinted with permission from [295]. Copyright 2023 Wiley VCH.

MOF and COF nanoarchitectonics approaches are excellent methods for rationally designing and building material structures from unit molecules and ions. Compared to conventional material synthesis methods, MOF and COF have a short history of development and leave plenty of room for various developments. The excellent dimensionality controlled nanoarchitectonics method is expected to contribute to the development of various functional systems.

#### 4. 2D to 3D Functional Amplification: Cells Regulated by the Surface

Within living cells, various functional units function through cascade-like coordination. Thus, external stimuli and molecular inputs often lead to sophisticated functions. This can be a useful system for linking two-dimensional nanoarchitectonics to three-dimensional function. Thus, creating artificial structures in two dimensions and altering the function of the cells that come into contact with them can be very sophisticated transfer from two-dimensional to three-dimensional nanoarchitectonics function. This section presents examples of cellular control by two-dimensional liquid interfaces and nanoarchitectonized two-dimensional structures.

Cells are cultured on solid interfaces such as conventional culture media. In the culture process, cells are affected by the solid surface of the equipment, such as mechanical properties. On the other hand, cell control at the liquid interface, which is unaffected by materials such as containers, is a pioneer area. In fact, liquid interfaces are found in many places as adaptive systems in biological systems, from the tear film of the eye to the liquid

lining of the lungs and stomach. At such interfaces, liquid interfaces are ubiquitous in natural adaptive systems. The fluidity and reconfigurability of liquids allow for unique response mechanisms. By anchoring living cells at the liquid interface, a system can be constructed that dynamically adapts to the forces generated by the cells. Such cell research at the soft liquid interface is attracting increasing attention. Jia et al. have successfully developed a technique that uses the interface between two immiscible liquids, aqueous cell culture solutions and perfluorocarbons, as a site for culturing and inducing differentiation of human mesenchymal stem cells (hMSCs) (Figure 16) [296]. At this interface, coexisting fibronectin proteins form organized nanosheets that exhibit transient mechanical effects with the cells. Early in culture, the traction force of the cells dynamically transformed the two-dimensional protein nanosheet into a hierarchical fiber structure. Elongated fibronectin aggregates modulate the size and elongation of the focal adhesions of the interacting network. Ultimately, these mechano-transduction signals determine the fate of stem cell differentiation. In this system, cultured hMSCs spontaneously differentiated into neurons without the addition of differentiation-inducing factors. The hMSCs adhered to the liquid interface and took an elongated adherent shape. Stress fibers of F-actin originating there were formed. The accumulation of downstream signaling protein phosphatase (FAK) activators in adhesion plaques and nuclear migration of Yes-associated protein (YAP) were also observed. hMSCs do not perceive protein nanosheets as soft, suggesting that some novel mechano-sensing mechanism is involved. Depending on the design of the two-dimensional nanoarchitectonics, it may be possible to induce differentiation into various types of cells, not only neural cells. This methodology is expected to lead to the development of new technologies for regenerative medicine.

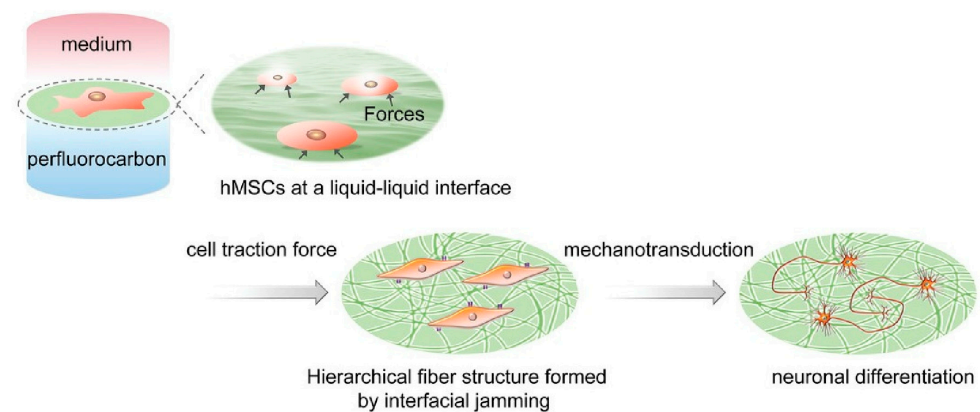


**Figure 16.** A technique that uses the interface between two immiscible liquids, aqueous cell culture solutions and perfluorocarbons, as a site for culturing and inducing differentiation of human mesenchymal stem cells (hMSCs). Reprinted with permission from [296]. Copyright 2019 Wiley VCH.

Protein nanofibrils are polymeric  $\beta$ -sheet aggregates of proteins of several microns in length. This structure is also a promising material to mimic extracellular matrix (ECM) matrix fibers due to its biocompatibility for cell adhesion and high mechanical strength. Jia et al. created an adaptive biomaterial based on a two-dimensional network of protein nanofibrils at the liquid–liquid interface and cultured hMSCs [297]. Culture on a two-dimensional network of protein nanofibrils at the liquid–liquid interface promoted neural differentiation of hMSCs. Throughout the study, lipid raft microdomains were found to play a central regulatory role in both the initial cell adhesion and subsequent neural differentiation of hMSCs (Figure 17). They are receptive to biophysical stimuli involving the lipid raft/focal adhesion kinase (FAK) pathway. It seems to direct the neural differentiation of hMSCs. Lipid rafts internalize cell adhesion molecules. In addition, lipid rafts act as an enrichment platform. This induces the integration of large signaling complexes. Through these processes, cells can rapidly adapt to the constantly changing microenvironment. FAK is one of the key mechano-sensors at the adaptive liquid interface. Spatiotemporal regula-

tion of FAK phosphorylation is a prerequisite for neural differentiation of hMSCs. Lipid raft formation and FAK phosphorylation at the adaptive liquid interface regulate hMSC differentiation. These findings also provide a better understanding of the fundamentals of cell-ECM dynamic interactions. Two-dimensional nanoarchitectonics can also incorporate bioactive proteins and responsive polymers. Two-dimensional nanoarchitectonics of liquid interfaces may provide opportunities to design adaptive biomaterials that were previously unimaginable.

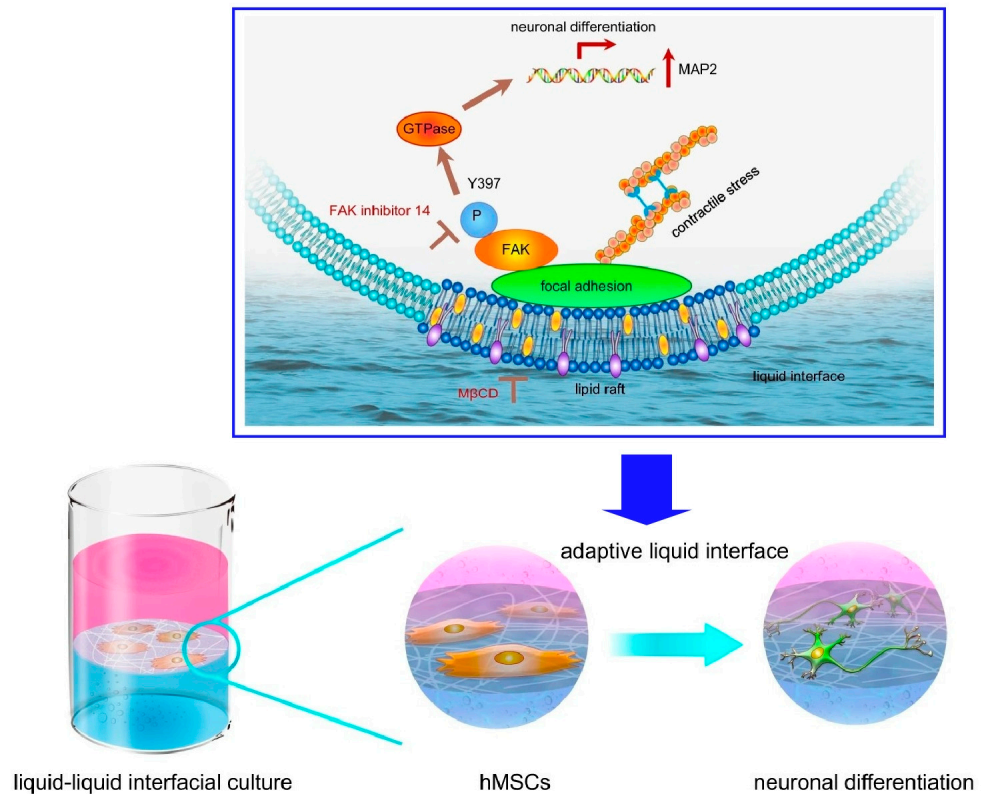


**Figure 17.** Culture on a two-dimensional network of protein nanofibrils at the liquid–liquid interface for neural differentiation of hMSCs where lipid raft microdomains were found to play a central regulatory role in both the initial cell adhesion and subsequent neural differentiation of hMSCs. Reproduced under terms of the CC-BY license [297]. Copyright 2022 Springer-Nature.

Gautrot and co-workers examine the interfacial dynamics of bovine serum albumin (BSA) and  $\beta$ -lactoglobulin (BLG) aggregates at the fluorinated liquid-water interface (Figure 18) [298]. The design of protein nanosheets based on these two globular proteins biofunctionalized with RGDSP peptides that enable cell adhesion is mentioned. High cell proliferation can be achieved even on bioemulsions with protein nanosheet formation without surfactants. As a strategy for the rational design of scaffold proteins at liquid interfaces, the fabrication of interfaces with strong shear dynamics and elasticity, bioactivity, and cell adhesion was investigated. For example, in the case of BLG nanosheets, relatively high elasticity was observed even in the absence of the co-surfactant. Based on this as well, the research demonstrated adhesion and proliferation of mesenchymal stem cells and human embryonic kidney (HEK) cells on bioemulsions stabilized with RGD-functionalized protein nanosheets. Such protein nanosheets and bioemulsions are useful for the development of bioreactors for scale-up of cell production. Such studies could also lead to the control of biological activity with scaffold proteins commonly used in food processing and stem cell technology, without the use of surfactant molecules.

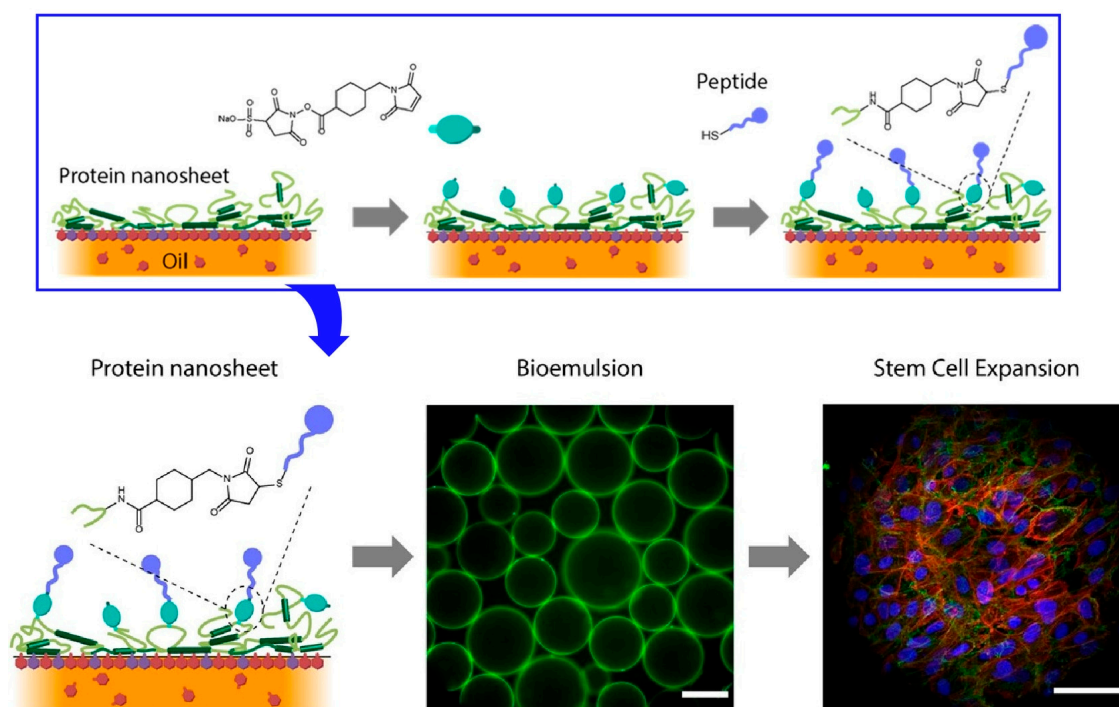


**Figure 18.** Interfacial dynamics of bovine serum albumin (BSA) and  $\beta$ -lactoglobulin (BLG) aggregates at the fluorinated liquid-water interface where high cell proliferation can be achieved even on bioemulsions with protein nanosheet formation without surfactants. Reproduced under terms of the CC-BY license [298]. Copyright 2023 American Chemical Society.

The use of liquid interfaces for cell culture has the potential to avoid the inconveniences of using solid substrates. In particular, it is advantageous in terms of scale-up and cell detachment. This methodology could be applied to other biotechnological platforms, such as microdroplet systems. For this purpose, analytical studies are needed. Gautrot and co-workers reconfirmed that cell spreading and growth on low-viscous liquid surfaces are enabled by the self-assembly of mechanically strong protein nanosheets at the interface [299]. Interfacial rheology and atomic force microscopy measurements revealed the mechanical properties of protein nanosheets and their associated liquid interfaces. The aggregation behavior of surfactant molecules with proteins and polymers associated at the liquid interface is directly related to the interfacial mechanics. Cells do not rely on surface tension to sustain diffusion, as in the case of amoebae, but primarily sense the in-plane mechanical properties of the interface (Figure 19). Based on these findings, it is essential to design bulk and nanoscale mechanical properties independently. Both scales can provide suitable structures and control cellular phenotypes. In other words, the design of biomaterials and implants requires nanoscale material design, where cell adhesion phenomena can be designed at the interface, independently of other bulk properties needed to provide flexibility and structure.

Gautrot and co-workers showed that mesenchymal and adherent stem cells can be cultured on liquid surfaces [300]. They also exemplified that this is mediated by the association of polymer nanosheets at the liquid-liquid interface. Despite the lack of bulk mechanical properties of the underlying liquid substrate, cell adhesion to the quasi-two-dimensional material is mediated by an integrin/actomyosin mechanism. Stem cell proliferation and differentiation are also controlled by the mechanical properties of the self-assembled protein nanosheets. Keratinocytes spread on rigid poly(l-lysine) nanosheets formed a structured actin cytoskeleton with distinct stress fibers. Focal adhesions were also formed. In contrast, cells adhering to the soft poly(l-lysine)-oil interface did not observe such structures. The

use of solid substrates often requires potentially harmful enzymatic degradation for cell recovery. The use of liquid substrates avoids such problems.

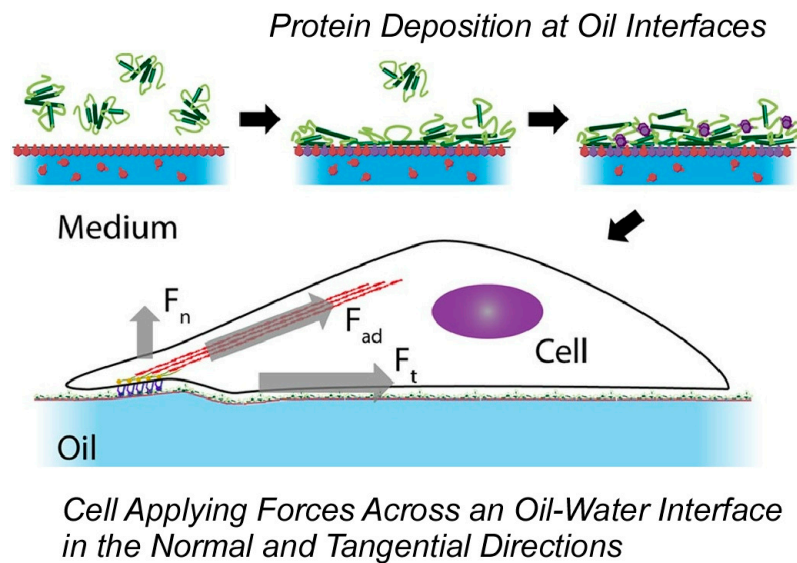


**Figure 19.** Cell spreading and growth on low-viscous liquid surfaces enabled by the self-assembly of mechanically strong protein nanosheets at the interface. Reproduced under terms of the CC-BY license [299]. Copyright 2018 American Chemical Society.

Cells are controlled not only by two-dimensional nanoarchitectonics, such as protein nanosheets that spontaneously form at the liquid interface, but also by the two-dimensional structure of artificially placed nanomaterials. For example, the assembly of fullerenes, which are nanomaterials of carbon materials, is often used in two-dimensional nanoarchitectonics. Although fullerenes are zero-dimensional spherical structures, they exhibit a variety of self-assembled structures from one dimension to three dimensions, such as sheets, rods, pores, and whiskers [301–309]. For example, fullerene nanowhiskers can be prepared on a large scale using the liquid–liquid interface deposition method. Minami and co-workers have successfully induced muscle differentiation by arranging fullerene nanowhiskers while simultaneously controlling the direction of cell growth (Figure 20) [310]. The two-dimensional in-plane aligned structure of fullerene nanowhiskers can be applied as a cell scaffold, and the orientation of muscle fibers formed during muscle differentiation can be controlled by the orientation of fullerene nanowhiskers. Using the Langmuir–Blodgett (LB) method, highly aligned one-dimensional fullerene nanowhiskey scaffolds were fabricated in the centimeter region. This scaffold can simultaneously control cell orientation and differentiation into muscle cells C2C12 myoblasts. Subsequently, myogenic differentiation and cell growth direction were analyzed by immunostaining for myosin heavy chain. A protein required for nucleus and myotube formation C2C12 myoblasts were found to fuse and form multinucleated myotubes. The fusion index increased from 12.3% on glass to 23.2% on aligned fullerene nanowhiskey scaffolds. One-dimensional fullerene nanowhiskers stimulate myoblast fusion. The direction of myotube formation strongly coincided with the direction of aligned fullerene nanowhiskers. When the same experiment was performed on bare glass, myoblasts fused randomly.

hMSCs are useful for cell-based tissue regeneration therapy because of their easy availability and potent immunosuppressive properties. However, the therapeutic efficacy based on hMSCs is limited by the small amount of human-derived cells isolated for clinical use. During *in vitro* growth, hMSCs undergo uncontrolled differentiation. In the process of *in vitro* proliferation, hMSCs undergo uncontrolled differentiation, thereby rapidly losing pluripotency and regenerative capacity. Therefore, new strategies to grow hMSCs *in vitro* while preserving their stem cell properties are strongly needed. This technique can produce large-area nanostructured surfaces with continuously adjustable alignment

of the constituents. Nanopatterned surfaces fabricated with high-aspect-ratio fullerene nanowhiskers could promote long-term pluripotency retention and differentiation potential of hMSCs via appropriate cell contractility and nuclear localization of Yes-associated protein (YAP) as demonstrated by Song et al. (Figure 21) [311]. Mechanical signals are transmitted to the nucleus by YAP. As a transcriptional coactivator, YAP translocation to the nucleus positively regulates the activity of core regulators (OCT4, SOX2, NANOG). As a result, retention of pluripotency of hMSCs is promoted. High aspect ratio fullerene nanowhiskers as cell culture scaffolds create an intermediate situation where focal adhesion is effectively reduced but not eliminated. As a result, long-term proliferation of hMSCs that retain pluripotency is mediated by appropriate cell contractility and nuclear localization of YAP. The pseudo-LB method used here is a simple technique that can be manipulated manually. It can be easily used to fabricate centimeter-sized nanopatterned substrates for the mass proliferation of hMSCs in clinical practice. This study demonstrates the importance of two-dimensional nanoarchitectonics for improving hMSCs technology in regenerative therapies.

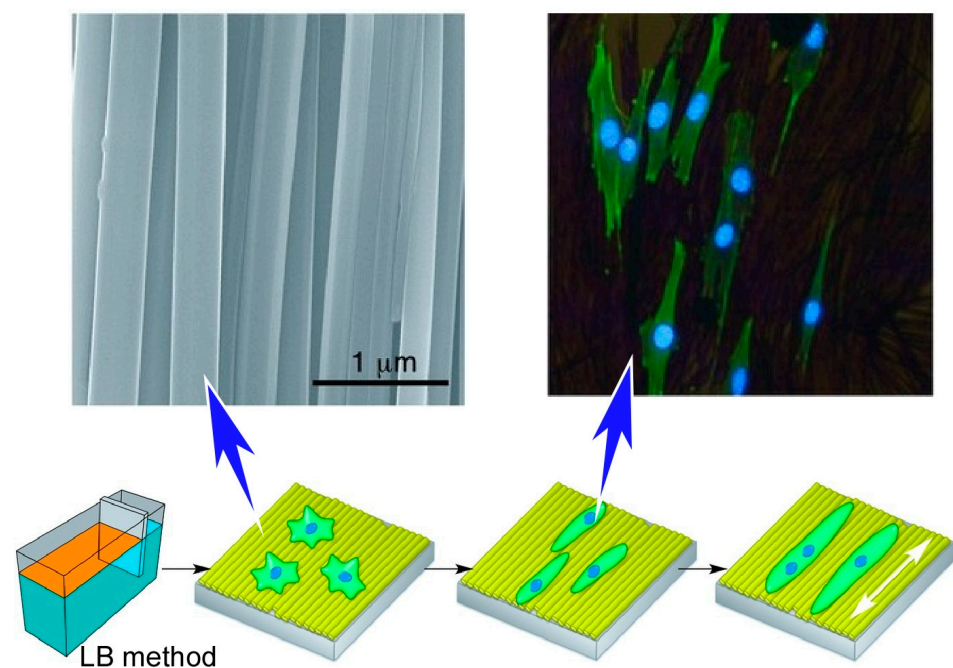


**Figure 20.** Muscle differentiation and simultaneously controlling the direction of cell growth on the two-dimensional in-plane aligned structure of fullerene nanowhiskers as a cell scaffold. Reprinted with permission from [310]. Copyright 2015 Wiley VCH.

Cells have well-developed cascade-like information transmission systems, which are excellent systems for generating large functions from simple stimuli. Exposing cells to structure-controlled two-dimensional surfaces allows for the expression of sophisticated functions such as cell differentiation and proliferation. Various scaffolds such as protein nanosheets and very rigid fullerene nanowhisker arrays, which form in very soft fields such as liquid surfaces, produce diverse cellular changes. This is not only of basic scientific interest as two-dimensional nanoarchitectonics makes a breakthrough into three-dimensional function. This is an area that should also make a significant contribution to practical areas such as regenerative medicine.

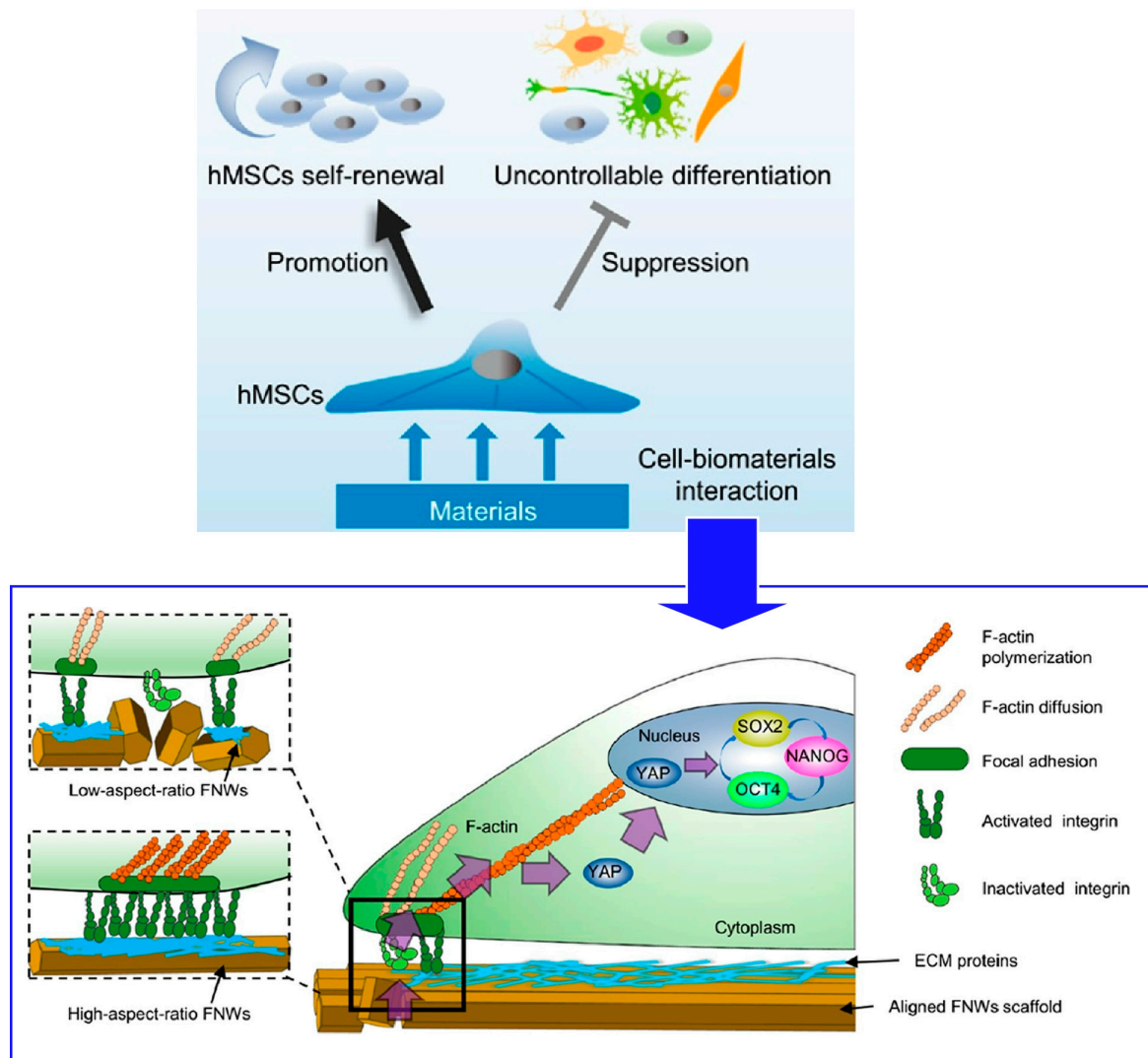


**Figure 21.** Nanopatterned surfaces fabricated with high-aspect-ratio fullerene nanowhiskers for long-term pluripotency retention and differentiation potential of hMSCs where mechanical signals are transmitted to the nucleus by YAP and YAP translocation to the nucleus positively regulates the activity of core regulators (OCT4, SOX2, NANOG). Reproduced under terms of the CC-BY license [311]. Copyright 2020 American Chemical Society.

## 5. Summary and Perspectives

Nanoarchitectonics is a post-nanotechnology concept that provides functional material systems from nano-units (atoms, molecules, and nanomaterials). Interfacial media contribute sufficiently to building functional materials. This is where two-dimensional (2D) materials as building units of three-dimensional (3D) functional nanoarchitectures are powerful. On top of that, materials nanoarchitectonics from two dimensions to three dimensions is necessary for the development of a wider range of functional materials. In this review, the control of liquid crystals from two dimensions, three-dimensional architecture of MOF/COF structures, and the control of cell arrangement and differentiation by two-dimensional contact are taken as examples.

Molecular films made of LB-type monolayers can control the orientation of liquid crystals as a command surface. The molecular-level phenomena of structural and orientation changes on the command surface are amplified into three-dimensional material properties such as liquid crystal orientation and phase transitions. This indicates that the combination of a soft oriented structure and a precise surface is useful. MOF and COF are methods that

enable rational design and construction of material structures from unit molecules and ions. The structure produced is determined by the arrangement of interacting functional groups in the molecular unit and the coordination structure of the ions. This means that the two-dimensional and three-dimensional structures of MOFs and COFs are determined by the structural design of the molecular unit-ion unit in the zero dimension. Therefore, the conversion from two dimensional to three dimensional can be achieved by devising the combination of the two-dimensional and three-dimensional structures. For structures with fixed interaction points, the structural design of the units is shown to be useful. Organisms are complex complexes of functions. However, cells have well-developed cascade-like information transmission systems. By exposing cells to structure-controlled two-dimensional surfaces, sophisticated functions such as cell differentiation and proliferation are expressed. This is a rational system for generating large three-dimensional functions from simple stimuli from two dimensions. Utilizing the cascade stimulus transduction system of living organisms is also useful for generating three-dimensional functions from two-dimensional nanoarchitectonics. In addition to approaches and examples described in this review article, simulations/theoretical perspective of 2D materials nanoarchitectonics for 3D functionalities are crucial matters. For example, both DFT calculation [312] and ab initio molecular dynamics [313] are rapidly transforming the field. With the aids of experimental and theoretical considerations, representative differences between 2D and 3D materials will be more clearly elucidated. Such additional efforts would lead to more sophisticated transformation from 2D to 3D from viewviewpoints of applications.

The several examples presented here have extracted several keys to increasing two-dimensional nanoarchitectonics to three-dimensional functionality. These include the use of soft orientation systems, the use of structural architecture reflecting molecular unit structures, and the use of cascade-like function transfer systems in living organisms. These are typical examples, but there may be other ways to link two-dimensional nanoarchitectonics to three-dimensional functionality. The ultimate goal of nanoarchitectonics is to create bio-like functional materials whose functions are hierarchical and exhibit complex interactions. Therefore, we must consider systems that incorporate multiple and diverse multifunctional mechanisms in three-dimension as described above. There are an infinite number of choices of substances, actions, and functions, and their combinations are also diverse. Therefore, there may be a limit to the trial-and-error or few-theory-based approach. Fortunately, humankind has developed artificial intelligence technology. In the field of materials science, machine learning approaches [314–316] and the concept of materials informatics [317–319] are being used. The combination of nanoarchitectonics and materials informatics has also been proposed [320,321]. The fabrication of functional structures from a large number of options may be completed with the help of artificial intelligence under the concept of nanoarchitectonics. Finally, these developments are expected to become nanoarchitectonics as a method for everything in materials science.

**Funding:** This study was partially supported by JSPS KAKENHI, grant number JP20H00392 and JP23H05459.

**Institutional Review Board Statement:** Not applicable.

**Informed Consent Statement:** Not applicable.

**Data Availability Statement:** Data sharing not applicable.

**Conflicts of Interest:** The author declares no conflict of interest.

## References

1. Liu, J.; Zhang, J.-G.; Yang, Z.; Lemmon, J.P.; Imhoff, C.; Graff, G.L.; Li, L.; Hu, J.; Wang, C.; Xiao, J.; et al. Materials science and materials chemistry for large scale electrochemical energy storage: From transportation to electrical grid. *Adv. Funct. Mater.* **2013**, *23*, 929–946. [[CrossRef](#)]
2. Kageyama, H.; Hayashi, K.; Maeda, K.; Attfield, J.P.; Hiroi, Z.; Rondinelli, J.M.; Poeppelmeier, K.R. Expanding frontiers in materials chemistry and physics with multiple anions. *Nat. Commun.* **2018**, *9*, 772. [[CrossRef](#)] [[PubMed](#)]

3. Kudo, A.; Miseki, Y. Heterogeneous photocatalyst materials for water splitting. *Chem. Soc. Rev.* **2009**, *38*, 253–278. [[CrossRef](#)] [[PubMed](#)]
4. Guo, D.; Shibuya, R.; Akiba, C.; Saji, S.; Kondo, T.; Nakamura, J. Active sites of nitrogen-doped carbon materials for oxygen reduction reaction clarified using model catalysts. *Science* **2016**, *351*, 361–365. [[CrossRef](#)] [[PubMed](#)]
5. Nandihalli, N.; Liu, C.J.; Mori, T. Polymer based thermoelectric nanocomposite materials and devices: Fabrication and characteristics. *Nano Energy* **2020**, *78*, 105186. [[CrossRef](#)]
6. Zhang, E.; Zhu, Q.; Huang, J.; Liu, J.; Tan, G.; Sun, C.; Li, T.; Liu, S.; Li, Y.; Wang, H.; et al. Visually resolving the direct Z-scheme heterojunction in CdS@ZnIn<sub>2</sub>S<sub>4</sub> hollow cubes for photocatalytic evolution of H<sub>2</sub> and H<sub>2</sub>O<sub>2</sub> from pure water. *Appl. Catal. B Environ.* **2021**, *293*, 120213. [[CrossRef](#)]
7. Qi, Y.; Zhang, J.; Kong, Y.; Zhao, Y.; Chen, S.; Li, D.; Liu, W.; Chen, Y.; Xie, T.; Cui, J.; et al. Unraveling of cocatalysts photodeposited selectively on facets of BiVO<sub>4</sub> to boost solar water splitting. *Nat. Commun.* **2022**, *13*, 484. [[CrossRef](#)]
8. Maeda, K.; Takeiri, F.; Kobayashi, G.; Matsuiishi, S.; Ogino, H.; Ida, S.; Mori, T.; Uchimoto, Y.; Tanabe, S.; Hasegawa, T.; et al. Recent progress on mixed-anion materials for energy applications. *Bull. Chem. Soc. Jpn.* **2022**, *95*, 26–37. [[CrossRef](#)]
9. Klyndyuk, A.I.; Chizhova, E.A.; Kharytonau, D.S.; Medvedev, D.A. Layered oxygen-deficient double perovskites as promising cathode materials for solid oxide fuel cells. *Materials* **2022**, *15*, 141. [[CrossRef](#)]
10. Jakhar, M.; Kumar, A.; Ahluwalia, P.K.; Tankeshwar, K.; Pandey, R. Engineering 2D materials for photocatalytic water-splitting from a theoretical perspective. *Materials* **2022**, *15*, 2221. [[CrossRef](#)]
11. Murugan, S.; Lee, E.-C. Recent Advances in the synthesis and application of vacancy-ordered halide double perovskite materials for solar cells: A promising alternative to lead-based perovskites. *Materials* **2023**, *16*, 5275. [[CrossRef](#)]
12. Desoky, M.M.H.; Caldera, F.; Brunella, V.; Ferrero, R.; Hoti, G.; Trotta, F. Cyclodextrins for lithium batteries applications. *Materials* **2023**, *16*, 5540. [[CrossRef](#)] [[PubMed](#)]
13. Pastuszak, J.; Węgierek, P. Photovoltaic cell generations and current research directions for their development. *Materials* **2022**, *15*, 5542. [[CrossRef](#)] [[PubMed](#)]
14. Tsuchii, Y.; Menda, T.; Hwang, S.; Yasuda, T. Photovoltaic properties of p-conjugated polymers based on fused cyclic imide and amide skeletons. *Bull. Chem. Soc. Jpn.* **2023**, *96*, 90–94. [[CrossRef](#)]
15. Yano, J.; Suzuk, K.; Hashimoto, C.; Tsutsumi, C.; Hayase, N.; Kitani, A. Trial fabrication of NADH-dependent enzymatic ethanol biofuel cell providing H<sub>2</sub> gas as well as Electricity. *Bull. Chem. Soc. Jpn.* **2023**, *96*, 331–338. [[CrossRef](#)]
16. Imahori, H. Molecular photoinduced charge separation: Fundamentals and application. *Bull. Chem. Soc. Jpn.* **2023**, *96*, 339–352. [[CrossRef](#)]
17. Chen, K.; Xiao, J.; Vequizo, J.J.M.; Hisatomi, T.; Ma, Y.; Nakabayashi, M.; Takata, T.; Yamakata, A.; Shibata, N.; Domen, K. Overall water splitting by a SrTaO<sub>2</sub>N-based photocatalyst decorated with an Ir-promoted Ru-based cocatalyst. *J. Am. Chem. Soc.* **2023**, *145*, 3839–3843. [[CrossRef](#)] [[PubMed](#)]
18. Huang, G.; Hu, M.; Xu, X.; Allothman, A.A.; Mushab, M.S.S.; Ma, S.; Shen, P.K.; Zhu, J.; Yamauchi, Y. Optimizing heterointerface of Co<sub>2</sub>P–Co<sub>x</sub>O<sub>y</sub> Nanoparticles within a porous carbon network for deciphering superior water splitting. *Small Struct.* **2023**, *4*, 2200235. [[CrossRef](#)]
19. Komaba, S.; Hasegawa, T.; Dahbi, M.; Kubota, K. Potassium intercalation into graphite to realize high-voltage/high-power potassium-ion batteries and potassium-ion capacitors. *Electrochem. Commun.* **2015**, *60*, 172–175. [[CrossRef](#)]
20. Saidul Islam, M.S.; Shudo, Y.; Hayami, S. Energy conversion and storage in fuel cells and super-capacitors from chemical modifications of carbon allotropes: State-of-art and prospect. *Bull. Chem. Soc. Jpn.* **2022**, *95*, 1–25. [[CrossRef](#)]
21. Yoshino, A. The lithium-ion battery: Two breakthroughs in development and two reasons for the Nobel Prize. *Bull. Chem. Soc. Jpn.* **2022**, *95*, 195–197. [[CrossRef](#)]
22. Kumar, R.; Joanni, E.; Sahoo, S.; Shim, J.-J.; Tan, W.K.; Matsuda, A.; Singh, R.K. An overview of recent progress in nanostructured carbon-based supercapacitor electrodes: From zero to bi-dimensional materials. *Carbon* **2022**, *193*, 298–338. [[CrossRef](#)]
23. Kumar, R.; Youssry, S.M.; Joanni, E.; Sahoo, S.; Kawamura, G.; Matsuda, A. Microwave-assisted synthesis of iron oxide homogeneously dispersed on reduced graphene oxide for high-performance supercapacitor electrodes. *J. Energy Storage* **2022**, *56*, 105896. [[CrossRef](#)]
24. Das, H.T.; Dutta, S.; Balaji, T.E.; Das, N.; Das, P.; Dheer, N.; Kanojia, R.; Ahuja, P.; Ujjain, S.K. Recent trends in carbon nanotube electrodes for flexible supercapacitors: A review of smart energy storage device assembly and performance. *Chemosensors* **2022**, *10*, 223. [[CrossRef](#)]
25. Kim, E.J.; Kumar, P.R.; Gossage, Z.T.; Kubota, K.; Hosaka, T.; Tatara, R.; Komaba, S. Active material and interphase structures governing performance in sodium and potassium ion batteries. *Chem. Sci.* **2022**, *13*, 6121–6158. [[CrossRef](#)] [[PubMed](#)]
26. Zhang, G.; QiuHong Bai, Q.; Wang, X.; Li, C.; Uyama, H.; Shen, Y. Preparation and mechanism investigation of walnut shell-based hierarchical porous carbon for supercapacitors. *Bull. Chem. Soc. Jpn.* **2023**, *96*, 190–197. [[CrossRef](#)]
27. Fu, M.; Chen, W.; Lei, Y.; Yu, H.; Lin, Y.; Terrones, M. Biomimetic construction of ferrite quantum dot/graphene heterostructure for enhancing ion/charge transfer in supercapacitors. *Adv. Mater.* **2023**, *35*, 2300940. [[CrossRef](#)] [[PubMed](#)]
28. Ganesan, P.; Ishihara, A.; Staykov, A.; Nakashima, N. Recent advances in nanocarbon-based nonprecious metal catalysts for oxygen/hydrogen reduction/evolution reactions and Zn-air battery. *Bull. Chem. Soc. Jpn.* **2023**, *96*, 429–443. [[CrossRef](#)]

29. Qiu, Y.-F.; Murayama, H.; Fujitomo, C.; Kawai, S.; Haruta, A.; Hiasa, T.; Mita, H.; Motohashi, K.; Yamamoto, E.; Tokunaga, M. Oxidative decomposition mechanism of ethylene carbonate on positive electrodes in lithium-ion batteries. *Bull. Chem. Soc. Jpn.* **2023**, *96*, 444–451. [[CrossRef](#)]
30. Lakshmi, K.C.S.; Vedhanarayanan, B. High-performance supercapacitors: A comprehensive review on paradigm shift of conventional energy storage devices. *Batteries* **2023**, *9*, 202. [[CrossRef](#)]
31. Honda, M.; Suzuki, N. Toxicities of polycyclic aromatic hydrocarbons for aquatic animals. *Int. J. Environ. Res. Public Health* **2020**, *17*, 1363. [[CrossRef](#)] [[PubMed](#)]
32. Qaidi, S.; Najm, H.M.; Abed, S.M.; Özkılıç, Y.O.; Al Dughaiishi, H.; Alost, M.; Sabri, M.M.S.; Alkhatib, F.; Milad, A. Concrete containing waste glass as an environmentally friendly aggregate: A review on fresh and mechanical characteristics. *Materials* **2022**, *15*, 6222. [[CrossRef](#)] [[PubMed](#)]
33. Li, S.L.; Chang, G.; Huang, Y.; Kinooka, K.; Chen, Y.; Fu, W.; Gong, G.; Yoshioka, T.; McKeown, N.B.; Hu, Y. Biphenol-based ultrathin microporous nanofilms for highly efficient molecular sieving separation. *Angew. Chem. Int. Ed.* **2022**, *61*, e202212816. [[CrossRef](#)]
34. Kushida, W.; Gonzales, R.R.; Shintani, T.; Matsuoka, A.; Nakagawa, K.; Yoshioka, T.; Hideto Matsuyama, H. Organic solvent mixture separation using fluorine-incorporated thin film composite reverse osmosis membrane. *J. Mater. Chem. A* **2022**, *10*, 4146–4156. [[CrossRef](#)]
35. Wang, X.; Liu, Z.; Lu, J.; Teng, H.; Fukuda, H.; Qin, W.; Wei, T.; Liu, Y. Highly selective membrane for efficient separation of environmental determinands: Enhanced molecular imprinting in polydopamine-embedded porous sleeve. *Chem. Eng. J.* **2022**, *449*, 137825. [[CrossRef](#)]
36. Zhang, L.; Chong, H.L.H.; Moh, P.Y.; Albaqami, M.D.; Tighezza, A.M.; Qin, C.; Ni, X.; Cao, J.; Xu, X.; Yamauchi, Y.  $\beta$ -FeOOH nanospindles as chloride-capturing electrodes for electrochemical faradic deionization of saline water. *Bull. Chem. Soc. Jpn.* **2023**, *96*, 306–309. [[CrossRef](#)]
37. Zhang, T.; Cain, A.K.; Semenec, L.; Liu, L.; Hosokawa, Y.; Inglis, D.W.; Yalikul, Y.; Li, M. Microfluidic separation and enrichment of *Escherichia coli* by size using viscoelastic flows. *Anal. Chem.* **2023**, *95*, 2561–2569. [[CrossRef](#)]
38. Chowdhury, R.; Al Biruni, M.T.; Afia, A.; Hasan, M.; Islam, M.R.; Ahmed, T. Medical waste incineration fly ash as a mineral filler in dense bituminous course in flexible pavements. *Materials* **2023**, *16*, 5612. [[CrossRef](#)]
39. Saleh, T.S.; Badawi, A.K.; Salama, R.S.; Mostafa, M.M.M. Design and development of novel composites containing nickel ferrites supported on activated carbon derived from agricultural wastes and its application in water remediation. *Materials* **2023**, *16*, 2170. [[CrossRef](#)]
40. Yadav, A.A.; Hunge, Y.M.; Kang, S.-W.; Fujishima, A.; Terashima, C. Enhanced photocatalytic degradation activity using the  $V_2O_5$ /RGO Composite. *Nanomaterials* **2023**, *13*, 338. [[CrossRef](#)]
41. Muradov, N.Z.; Veziroğlu, T.N. “Green” path from fossil-based to hydrogen economy: An overview of carbon-neutral technologies. *Int. J. Hydrogen Energy* **2008**, *33*, 6804–6839. [[CrossRef](#)]
42. Chen, S.; Liu, J.; Zhang, Q.; Teng, F.; McLellan, B.C. A critical review on deployment planning and risk analysis of carbon capture, utilization, and storage (CCUS) toward carbon neutrality. *Renew. Sust. Energ. Rev.* **2022**, *167*, 112537. [[CrossRef](#)]
43. Chapman, A.; Kubota, E.; Kubota, M.; Nagao, A.; Bertsch, K.; Macadre, A.; Tsuchiyama, T.; Masamura, T.; Takaki, S.; Komoda, R.; et al. Achieving a carbon neutral future through advanced functional materials and technologies. *Bull. Chem. Soc. Jpn.* **2022**, *95*, 73–103. [[CrossRef](#)]
44. Li, Y.; Ma, G. A Study on the high-quality development path and implementation countermeasures of China’s construction industry toward the carbon peaking and carbon neutralization goals. *Sustainability* **2024**, *16*, 772. [[CrossRef](#)]
45. Takeishi, K. Evolution of turbine cooled vanes and blades applied for large industrial gas turbines and its trend toward carbon neutrality. *Energies* **2022**, *15*, 8935. [[CrossRef](#)]
46. Takase, S.; Aritsu, T.; Sakamoto, Y.; Sakuno, Y.; Shimizu, Y. Preparation of highly conductive phthalocyaninato-cobalt iodide at the interface between aqueous KI solution and organic solvent and catalytic properties for electrochemical reduction of  $CO_2$ . *Bull. Chem. Soc. Jpn.* **2023**, *96*, 649–653. [[CrossRef](#)]
47. Ishihara, S.; O’Kelly, C.J.; Takeshi Tanaka, T.; Kataura, H.; Labuta, J.; Shingaya, Y.; Nakayama, T.; Ohsawa, T.; Nakanishi, T.; Swager, T.M. Metallic versus semiconducting SWCNT chemiresistors: A case for separated SWCNTs wrapped by a metallosupramolecular polymer. *ACS Appl. Mater. Interfaces* **2017**, *9*, 38062–38067. [[CrossRef](#)]
48. Sasaki, Y.; Kubota, R.; Minami, T. Molecular self-assembled chemosensors and their arrays. *Coord. Chem. Rev.* **2021**, *429*, 213607. [[CrossRef](#)]
49. Masuda, Y. Recent advances in  $SnO_2$  nanostructure based gas sensors. *Sens. Actuat. B Chem.* **2022**, *364*, 131876. [[CrossRef](#)]
50. Tatli, S.; Mirzaee-Ghaleh, E.; Rabbani, H.; Karami, H.; Wilson, A.D. Rapid Detection of Urea Fertilizer Effects on VOC Emissions from Cucumber Fruits Using a MOS E-Nose Sensor Array. *Agronomy* **2022**, *12*, 35. [[CrossRef](#)]
51. Saito, S.; Haraga, T.; Marumo, K.; Sato, Y.; Nakano, Y.; Tasaki-Handa, Y.; Shibukawa, M. Americium(III)/curium(III) complete separation and sensitive fluorescence detection by capillary and gel electrophoresis using emissive hexadentate/octadentate polyaminocarboxylate ligands. *Bull. Chem. Soc. Jpn.* **2023**, *96*, 223–225. [[CrossRef](#)]
52. Simonenko, N.P.; Glukhova, O.E.; Plugin, I.A.; Kolosov, D.A.; Nagornov, I.A.; Simonenko, T.L.; Varezchnikov, A.S.; Simonenko, E.P.; Sysoev, V.V.; Kuznetsov, N.T. The  $Ti_0.2V_1.8C$  MXene ink-prepared chemiresistor: From theory to tests with humidity versus VOCs. *Chemosensors* **2023**, *11*, 7. [[CrossRef](#)]

53. Dong, L.; Wang, M.; Wu, J.; Zhu, C.; Shi, J.; Morikawa, H. Stretchable, adhesive, self-healable, and conductive hydrogel-based deformable triboelectric nanogenerator for energy harvesting and human motion sensing. *ACS Appl. Mater. Interfaces* **2022**, *14*, 9126–9137. [[CrossRef](#)]
54. Anggraini, L.E.; Rahmawati, H.; Nasution, M.A.F.; Jiwanti, P.K.; Einaga, Y.; Ivandini, T.A. Development of an acrylamide biosensor using guanine and adenine as biomarkers at boron-doped diamond electrodes: Integrated molecular docking and experimental studies. *Bull. Chem. Soc. Jpn.* **2023**, *96*, 420–428. [[CrossRef](#)]
55. Kalyana Sundaram, S.d.; Hossain, M.M.; Rezki, M.; Ariga, K.; Tsujimura, S. Enzyme cascade electrode reactions with nanomaterials and their applicability towards biosensor and biofuel cells. *Biosensors* **2023**, *13*, 1018. [[CrossRef](#)] [[PubMed](#)]
56. Lostao, A.; Lim, K.S.; Pallarés, M.C.; Ptak, A.; Marcuello, C. Recent advances in sensing the inter-biomolecular interactions at the nanoscale—A comprehensive review of AFM-based force spectroscopy. *Int. J. Biol. Macromol.* **2023**, *238*, 124089. [[CrossRef](#)] [[PubMed](#)]
57. Theyagarajan, K.; Kim, Y.-J. Recent Developments in the Design and Fabrication of Electrochemical Biosensors Using Functional Materials and Molecules. *Biosensors* **2023**, *13*, 424. [[CrossRef](#)]
58. Bhaskar, S. Biosensing Technologies: A Focus Review on Recent Advancements in Surface Plasmon Coupled Emission. *Micromachines* **2023**, *14*, 574. [[CrossRef](#)]
59. Cabral, H.; Miyata, K.; Osada, K.; Kataoka, K. Block copolymer micelles in nanomedicine applications. *Chem. Rev.* **2018**, *118*, 6844–6892. [[CrossRef](#)] [[PubMed](#)]
60. Rabiee, N.; Ahmadi, S.; Akhavan, O.; Luque, R. Silver and gold nanoparticles for antimicrobial purposes against multi-drug resistance bacteria. *Materials* **2022**, *15*, 1799. [[CrossRef](#)]
61. Naganthran, A.; Verasoundarapandian, G.; Khalid, F.E.; Masarudin, M.J.; Zulkharnain, A.; Nawawi, N.M.; Karim, M.; Che Abdullah, C.A.; Ahmad, S.A. Synthesis, characterization and biomedical application of silver nanoparticles. *Materials* **2022**, *15*, 427. [[CrossRef](#)]
62. Bhattacharya, T.; Soares, G.A.B.e.; Chopra, H.; Rahman, M.M.; Hasan, Z.; Swain, S.S.; Cavalu, S. Applications of phytonanotechnology for the treatment of neurodegenerative disorders. *Materials* **2022**, *15*, 804. [[CrossRef](#)]
63. Islam, F.; Shohag, S.; Uddin, M.J.; Islam, M.R.; Nafady, M.H.; Akter, A.; Mitra, S.; Roy, A.; Emran, T.B.; Cavalu, S. Exploring the journey of zinc oxide nanoparticles (ZnO-NPs) toward biomedical applications. *Materials* **2022**, *15*, 2160. [[CrossRef](#)]
64. Komiyama, M. Molecular mechanisms of the medicines for COVID-19. *Bull. Chem. Soc. Jpn.* **2022**, *95*, 1308–1317. [[CrossRef](#)]
65. Quader, S.; Kataoka, K.; Cabral, H. Nanomedicine for brain cancer. *Adv. Drug Deliv. Rev.* **2022**, *182*, 114115. [[CrossRef](#)]
66. Yokoo, H.; Oba, M.; Uchida, S. Cell-penetrating peptides: Emerging tools for mRNA delivery. *Pharmaceutics* **2022**, *14*, 78. [[CrossRef](#)] [[PubMed](#)]
67. Younis, M.A.; Sato, Y.; Elewa, Y.H.A.; Kon, Y.; Harashima, H. Self-homing nanocarriers for mRNA delivery to the activated hepatic stellate cells in liver fibrosis. *J. Control Release* **2023**, *353*, 685–698. [[CrossRef](#)] [[PubMed](#)]
68. Rajan, R.; Kumar, N.; Zhao, D.; Dai, X.; Kawamoto, K.; Matsumura, K. Polyampholyte-based polymer hydrogels for the long-term storage, protection and delivery of therapeutic proteins. *Adv. Healthcare Mater.* **2023**, *12*, 2203253. [[CrossRef](#)] [[PubMed](#)]
69. Khan, M.S.; Baskoy, S.A.; Yang, C.; Hong, J.; Chae, J.; Ha, H.; Lee, S.; Tanaka, M.; Choi, Y.; Choi, J. Lipid-based colloidal nanoparticles for applications in targeted vaccine delivery. *Nanoscale Adv.* **2023**, *5*, 1853–1869. [[CrossRef](#)] [[PubMed](#)]
70. Minamiki, T.; Ichikawa, Y.; Kurita, R. The power of assemblies at interfaces: Nanosensor platforms based on synthetic receptor membranes. *Sensors* **2020**, *20*, 2228. [[CrossRef](#)] [[PubMed](#)]
71. Saito, Y.; Sasabe, H.; Tsuneyama, H.; Abe, S.; Matsuya, M.; Kawano, T.; Kori, Y.; Hanayama, T.; Kido, J. Quinoline-modified phenanthroline electron-transporters as n-type exciplex partners for highly efficient and stable deep-red OLEDs. *Bull. Chem. Soc. Jpn.* **2023**, *96*, 24–28. [[CrossRef](#)]
72. Matsuya, M.; Sasabe, H.; Sumikoshi, S.; Hoshi, K.; Nakao, K.; Kumada, K.; Sugiyama, R.; Sato, R.; Kido, J. Highly luminescent aluminum complex with  $\beta$ -diketone ligands exhibiting near-unity photoluminescence quantum yield, thermally activated delayed fluorescence, and rapid radiative decay rate properties in solution-processed organic light-emitting devices. *Bull. Chem. Soc. Jpn.* **2023**, *96*, 183–189. [[CrossRef](#)]
73. Maeki, M.; Uno, S.; Niwa, A.; Okada, Y.; Tokeshi, M. Microfluidic technologies and devices for lipid nanoparticle-based RNA delivery. *J. Control Release* **2022**, *344*, 80–96. [[CrossRef](#)]
74. Ishii, M.; Yamashita, Y.; Watanabe, S.; Ariga, K.; Takeya, J. Doping of molecular semiconductors through proton-coupled electron transfer. *Nature* **2023**, *622*, 285–291. [[CrossRef](#)]
75. Hatakeyama-Sato, K.; Oyaizu, K. Redox: Organic robust radicals and their polymers for energy conversion/storage devices. *Chem. Rev.* **2023**, *123*, 11336–11391. [[CrossRef](#)]
76. Jung, T.A.; Schlittler, R.R.; Gimzewski, J.K.; Tang, H.; Joachim, C. Controlled room-temperature positioning of individual molecules: Molecular flexure and motion. *Science* **1996**, *271*, 181–184. [[CrossRef](#)]
77. Sugimoto, Y.; Pou, P.; Abe, M.; Jelinek, P.; Pérez, R.; Morita, S.; Custance, Ó. Chemical identification of individual surface atoms by atomic force microscopy. *Nature* **2007**, *446*, 64–67. [[CrossRef](#)] [[PubMed](#)]
78. Kimura, K.; Miwa, K.; Imada, H.; Imai-Imada, M.; Kawahara, S.; Takeya, J.; Kawai, M.; Galperin, M.; Kim, Y. Selective triplet exciton formation in a single molecule. *Nature* **2019**, *570*, 210–213. [[CrossRef](#)] [[PubMed](#)]
79. Yamashita, Y.; Tsurumi, J.; Ohno, M.; Fujimoto, R.; Kumagai, S.; Kurosawa, T.; Okamoto, T.; Takeya, J.; Watanabe, S. Efficient molecular doping of polymeric semiconductors driven by anion exchange. *Nature* **2019**, *572*, 634–638. [[CrossRef](#)] [[PubMed](#)]

80. Soe, W.-H.; Srivastava, S.; Joachim, C. Train of single molecule-gears. *J. Phys. Chem. Lett.* **2019**, *10*, 6462–6467. [[CrossRef](#)] [[PubMed](#)]
81. Kawai, S.; Krejčí, O.; Nishiuchi, T.; Sahara, K.; Kodama, T.; Pawlak, R.; Meyer, E.; Kubo, T.; Foster, A.S. Three-dimensional graphene nanoribbons as a framework for molecular assembly and local probe chemistry. *Sci. Adv.* **2020**, *6*, eaay8913. [[CrossRef](#)]
82. Kawai, S.; Sang, H.; Kantorovich, L.; Takahashi, K.; Nozaki, K.; Ito, S. An endergonic synthesis of single Sondheimer–Wong diyne by local probe chemistry. *Angew. Chem. Int. Ed.* **2020**, *59*, 10842. [[CrossRef](#)]
83. Wooten, B.L.; Iguchi, R.; Tang, P.; Kang, J.S.; Uchida, K.; Bauer, G.E.W.; Heremans, J.P. Electric field-dependent phonon spectrum and heat conduction in ferroelectrics. *Sci. Adv.* **2021**, *9*, eadd7194. [[CrossRef](#)]
84. Liu, X.; Farahi, G.; Chiu, C.-L.; Papic, Z.; Watanabe, K.; Taniguchi, T.; Zaletel, M.P.; Yazdani, A. Visualizing broken symmetry and topological defects in a quantum Hall ferromagnet. *Science* **2022**, *375*, 321–326. [[CrossRef](#)]
85. Xing, J.; Takeuchi, K.; Kamei, K.; Nakamuro, T.; Harano, K.; Nakamura, E. Atomic-number (Z)-correlated atomic sizes for deciphering electron microscopic molecular images. *Proc. Natl. Acad. Sci. USA* **2022**, *119*, e2114432119. [[CrossRef](#)]
86. Matsuno, T.; Isobe, H. Trapped yet free inside the tube: Supramolecular chemistry of molecular peapods. *Bull. Chem. Soc. Jpn.* **2023**, *96*, 406–419. [[CrossRef](#)]
87. Itoh, T.; Procházka, M.; Dong, Z.-C.; Ji, W.; Yamamoto, Y.S.; Zhang, Y.; Ozaki, Y. Toward a new era of SERS and TERS at the nanometer scale: From fundamentals to innovative applications. *Chem. Rev.* **2023**, *123*, 1552–1634. [[CrossRef](#)] [[PubMed](#)]
88. Oyamada, N.; Minamimoto, H.; Fukushima, T.; Zhou, R.; Murakoshi, K. Beyond single-molecule chemistry for electrified interfaces using molecule polaritons. *Bull. Chem. Soc. Jpn.* **2024**, *97*, uoae007. [[CrossRef](#)]
89. Fan, L.-B.; Shu, C.-C.; Dong, D.; He, J.; Henriksen, N.E.; Nori, F. Quantum coherent control of a single molecular-polariton rotation. *Phys. Rev. Lett.* **2023**, *130*, 043604. [[CrossRef](#)] [[PubMed](#)]
90. Ariga, K. Nanoarchitectonics: What’s coming next after nanotechnology? *Nanoscale Horiz.* **2021**, *6*, 364–378. [[CrossRef](#)] [[PubMed](#)]
91. Feynman, R.P. There’s plenty of room at the bottom. *Calif. Inst. Technol. J. Eng. Sci.* **1960**, *4*, 23–36.
92. Roukes, M. Plenty of room, indeed. *Sci. Am.* **2001**, *285*, 48–57. [[CrossRef](#)]
93. Ariga, K.; Minami, K.; Ebara, M.; Nakanishi, J. What are the emerging concepts and challenges in NANO? Nanoarchitectonics, hand-operating nanotechnology and mechanobiology. *Polym. J.* **2016**, *48*, 371–389. [[CrossRef](#)]
94. Ariga, K. Chemistry of materials nanoarchitectonics for two-dimensional films: Langmuir–Blodgett, layer-by-layer assembly, and newcomers. *Chem. Mater.* **2023**, *35*, 5233–5254. [[CrossRef](#)]
95. Ariga, K.; Nishikawa, M.; Mori, T.; Takeya, J.; Shrestha, L.K.; Hill, J.P. Self-assembly as a key player for materials nanoarchitectonics. *Sci. Technol. Adv. Mater.* **2019**, *20*, 51–95. [[CrossRef](#)]
96. Cao, L.; Huang, Y.; Parakhonskiy, B.; Skirtach, A.G. Nanoarchitectonics beyond perfect order – not quite perfect but quite useful. *Nanoscale* **2022**, *14*, 15964–16002. [[CrossRef](#)]
97. Ariga, K. Liquid–liquid interfacial nanoarchitectonics. *Small* **2023**, 2305636. [[CrossRef](#)] [[PubMed](#)]
98. Ariga, K.; Li, J.; Fei, J.; Ji, Q.; Hill, J.P. Nanoarchitectonics for dynamic functional materials from atomic-/molecular-level manipulation to macroscopic action. *Adv. Mater.* **2016**, *28*, 1251–1286. [[CrossRef](#)]
99. Ariga, K.; Jia, X.; Song, J.; Hill, J.P.; Leong, D.T.; Jia, Y.; Li, J. Nanoarchitectonics beyond self-assembly: Challenges to create bio-like hierarchic organization. *Angew. Chem. Int. Ed.* **2020**, *59*, 15424–15446. [[CrossRef](#)] [[PubMed](#)]
100. Aono, M.; Ariga, K. The way to nanoarchitectonics and the way of nanoarchitectonics. *Adv. Mater.* **2016**, *28*, 989–992. [[CrossRef](#)] [[PubMed](#)]
101. Laughlin, R.B.; Pines, D. The theory of everything. *Proc. Natl. Acad. Sci. USA* **2000**, *97*, 28–31. [[CrossRef](#)]
102. Ariga, K.; Fakhrullin, R. Materials nanoarchitectonics from atom to living cell: A method for everything. *Bull. Chem. Soc. Jpn.* **2022**, *95*, 774–795. [[CrossRef](#)]
103. Ariga, K. Nanoarchitectonics: Method for everything in materials science. *Bull. Chem. Soc. Jpn.* **2024**, *97*, uoad001. [[CrossRef](#)]
104. Oaki, Y.; Sato, K. Nanoarchitectonics for conductive polymers using solid and vapor phases. *Nanoscale Adv.* **2022**, *4*, 2773–2781. [[CrossRef](#)] [[PubMed](#)]
105. Nguyen, N.T.; Lebastard, C.; Wilmet, M.; Dumait, N.; Renaud, A.; Cordier, S.; Ohashi, N.; Uchikoshi, T.; Grasset, F. A review on functional nanoarchitectonics nanocomposites based on octahedral metal atom clusters (Nb<sub>6</sub>, Mo<sub>6</sub>, Ta<sub>6</sub>, W<sub>6</sub>, Re<sub>6</sub>): Inorganic 0D and 2D powders and films. *Sci. Technol. Adv. Mater.* **2022**, *23*, 547–578. [[CrossRef](#)] [[PubMed](#)]
106. Datta, K.K.R. Exploring the self-cleaning facets of fluorinated graphene nanoarchitectonics: Progress and perspectives. *Chem-NanoMat* **2023**, *9*, e202300135. [[CrossRef](#)]
107. Zhang, Z.-P.; Xia, H. Nanoarchitectonics and applications of gallium-based liquid metal micro- and nanoparticles. *ChemNanoMat* **2023**, *9*, e202300078. [[CrossRef](#)]
108. Trifoi, A.R.; Matei, E.; Râpă, M.; Berbecaru, A.-C.; Panaitescu, C.; Banu, I.; Doukeh, R. Coprecipitation nanoarchitectonics for the synthesis of magnetite: A review of mechanism and characterization. *React. Kinet. Mech. Catal.* **2023**, *136*, 2835–2874. [[CrossRef](#)]
109. Guan, X.; Li, Z.; Geng, X.; Lei, Z.; Karakoti, A.; Wu, T.; Kumar, P.; Yi, J.; Vinu, A. Emerging trends of carbon-based quantum dots: Nanoarchitectonics and applications. *Small* **2023**, *19*, 2207181. [[CrossRef](#)]
110. Jiang, H.; Gao, J.; Zhang, X.; Guo, N. Composite micro-nanoarchitectonics of MMT-SiO<sub>2</sub>: Space charge characteristics under tensile state. *Polymers* **2021**, *13*, 4354. [[CrossRef](#)]
111. Chen, Q.; Li, H. Nanoarchitectonics of carbon nanostructures: Sodium dodecyl sulfonate @ sodium chloride system. *Nanomaterials* **2022**, *12*, 1652. [[CrossRef](#)]

112. Hakim, M.L.; Hanif, A.; Alam, T.; Islam, M.T.; Arshad, H.; Soliman, M.S.; Albadran, S.M.; Islam, M.S. Ultrawideband polarization-independent nanoarchitectonics: A perfect metamaterial absorber for visible and infrared optical window applications. *Nanomaterials* **2022**, *12*, 2849. [[CrossRef](#)]
113. Ling, L.; Wu, C.; Xing, F.; Memon, S.A.; Sun, H. Recycling nanoarchitectonics of graphene oxide from carbon fiber reinforced polymer by the electrochemical method. *Nanomaterials* **2022**, *12*, 3657. [[CrossRef](#)]
114. Tong, T.; Zhao, Y.; Wang, S.; Mo, D.; Deng, K.; Chao, P. Electropolymerization nanoarchitectonics of different bithiophene precursors for tuning optoelectronic performances of polythiophenes. *Mater. Chem. Phys.* **2024**, *311*, 128544. [[CrossRef](#)]
115. Ariga, K.; Shionoya, M. Nanoarchitectonics for coordination asymmetry and related chemistry. *Bull. Chem. Soc. Jpn.* **2021**, *94*, 839–859. [[CrossRef](#)]
116. Jia, J.; Wu, D.; Ren, Y.; Lin, J. Nanoarchitectonics of illite-based materials: Effect of metal oxides Intercalation on the mechanical properties. *Nanomaterials* **2022**, *12*, 997. [[CrossRef](#)]
117. Lin, Y.-F.; Lai, Y.-R.; Sung, H.-L.; Chung, T.-W.; Lin, K.-Y.A. Design of amine-modified Zr–Mg mixed oxide aerogel nanoarchitectonics with dual lewis acidic and basic sites for CO<sub>2</sub>/propylene oxide cycloaddition reactions. *Nanomaterials* **2022**, *12*, 3442. [[CrossRef](#)] [[PubMed](#)]
118. Zeng, L.; Liu, Z.; Huang, J.; Wang, X.; Guo, H.; Li, W.-H. Anti-fouling performance of hydrophobic hydrogels with unique surface hydrophobicity and nanoarchitectonics. *Gels* **2022**, *8*, 407. [[CrossRef](#)] [[PubMed](#)]
119. Qiu, Z.; Jinschek, J.R.; Gouma, P.-I. Two-step solvothermal process for nanoarchitectonics of metastable hexagonal WO<sub>3</sub> nanoplates. *Crystals* **2023**, *13*, 690. [[CrossRef](#)]
120. Zhang, X.; Yang, P. Role of graphitic carbon in g-C<sub>3</sub>N<sub>4</sub> nanoarchitectonics towards efficient photocatalytic reaction kinetics: A review. *Carbon* **2023**, *216*, 118584. [[CrossRef](#)]
121. Haketa, Y.; Yamasumi, K.; Maeda, H.  $\pi$ -Electronic ion pairs: Building blocks for supramolecular nanoarchitectonics via <sup>i</sup>p-<sup>i</sup>p interactions. *Chem. Soc. Rev.* **2023**, *52*, 7170–7196. [[CrossRef](#)] [[PubMed](#)]
122. Béres, K.A.; Homonnay, Z.; Bereczki, L.; Dürvanger, Z.; Petruševski, V.M.; Farkas, A.; Kótai, L. Crystal nanoarchitectonics and characterization of the octahedral iron(III)–nitrate complexes with isomer dimethylurea ligands. *Crystals* **2023**, *13*, 1019. [[CrossRef](#)]
123. Lahmidi, S.; Anouar, E.H.; Ettahiri, W.; El Hafi, M.; Lazrak, F.; Alanazi, M.M.; Alanazi, A.S.; Hefnawy, M.; Essassi, E.M.; Mague, J.T. Nanoarchitectonics and molecular docking of 4-(dimethylamino)pyridin-1-ium 2-3 methyl-4-oxo-pyri-do [1,2-*a*]pyrimidine-3-carboxylate. *Crystals* **2023**, *13*, 1333. [[CrossRef](#)]
124. Hecht, S. Welding, organizing, and planting organic molecules on substrate surfaces—Promising approaches towards nanoarchitectonics from the bottom up. *Angew. Chem. Int. Ed.* **2003**, *42*, 24–26. [[CrossRef](#)] [[PubMed](#)]
125. Musa, A.; Hakim, M.L.; Alam, T.; Islam, M.T.; Alshammari, A.S.; Mat, K.; Almalki, S.H.; Islam, M.S. Polarization independent metamaterial absorber with anti-reflection coating nanoarchitectonics for visible and infrared window applications. *Materials* **2022**, *15*, 3733. [[CrossRef](#)] [[PubMed](#)]
126. Ramanathan, M.; Shrestha, L.K.; Mori, T.; Ji, Q.; Hill, J.P.; Ariga, K. Amphiphile nanoarchitectonics: From basic physical chemistry to advanced applications. *Phys. Chem. Chem. Phys.* **2013**, *15*, 10580–10611. [[CrossRef](#)]
127. Hikichi, R.; Tokura, Y.; Igarashi, Y.; Imai, H.; Oaki, Y. Fluorine-free substrate-independent superhydrophobic Coatings by nanoarchitectonics of polydispersed 2D materials. *Bull. Chem. Soc. Jpn.* **2023**, *96*, 766–774. [[CrossRef](#)]
128. Xing, Z.; Zhang, C.; Xue, N.; Li, Z.; Li, F.; Wan, X.; Guo, S.; Hao, J. High-frequency surface insulation strength with nanoarchitectonics of disiloxane modified polyimide films. *Polymers* **2022**, *14*, 146. [[CrossRef](#)]
129. Conti Nibali, V.; D’Angelo, G.; Arena, A.; Ciofi, C.; Scandurra, G.; Branca, C. TiO<sub>2</sub> Nanoparticles dispersion in block-copolymer aqueous solutions: Nanoarchitectonics for self-assembly and aggregation. *J. Funct. Biomater.* **2022**, *13*, 39. [[CrossRef](#)]
130. Kim, D.; Gu, M.; Park, M.; Kim, T.; Kim, B.-S. Layer-by-layer assembly for photoelectrochemical nanoarchitectonics. *Mol. Syst. Des. Eng.* **2019**, *4*, 65–77. [[CrossRef](#)]
131. Zhang, L.; Wang, T.; Shen, Z.; Liu, M. Chiral nanoarchitectonics: Towards the design, self-assembly, and function of nanoscale chiral twists and helices. *Adv. Mater.* **2016**, *28*, 1044–1059. [[CrossRef](#)]
132. Marin, E.; Tapeinos, C.; Sarasua, J.R.; Larrañaga, A. Exploiting the layer-by-layer nanoarchitectonics for the fabrication of polymer capsules: A toolbox to provide multifunctional properties to target complex pathologies. *Adv. Colloid Interface Sci.* **2022**, *304*, 102680. [[CrossRef](#)] [[PubMed](#)]
133. Li, Z.; Zhao, C.; Lin, X.; Ouyang, G.; Liu, M. Stepwise solution-interfacial nanoarchitectonics for assembled film with full-color and white-light circularly polarized luminescence. *ACS Appl. Mater. Interfaces* **2023**, *15*, 31077–31086. [[CrossRef](#)]
134. Parbat, D.; Jana, N.; Dhar, M.; Mann, U. Reactive multilayer coating as versatile nanoarchitectonics for customizing various bioinspired liquid wettabilities. *ACS Appl. Mater. Interfaces* **2022**, *15*, 25232–25247. [[CrossRef](#)]
135. Huang, S.-Y.; Hsieh, P.-Y.; Chung, C.-J.; Chou, C.-M.; He, J.-L. Nanoarchitectonics for ultrathin gold films deposited on collagen fabric by high-power impulse magnetron sputtering. *Nanomaterials* **2022**, *12*, 1627. [[CrossRef](#)]
136. Wang, Y.; Niu, D.; Ouyang, G.; Liu, M. Double helical  $\pi$ -aggregate nanoarchitectonics for amplified circularly polarized luminescence. *Nat. Commun.* **2022**, *13*, 1710. [[CrossRef](#)] [[PubMed](#)]
137. Akamatsu, M. Inner and interfacial environmental nanoarchitectonics of supramolecular assemblies formed by amphiphiles: From emergence to application. *J. Oleo Sci.* **2023**, *72*, 105–116. [[CrossRef](#)] [[PubMed](#)]
138. Pahal, S.; Boranna, R.; Tripathy, A.; Goudar, V.S.; Veetil, V.T.; Kurapati, R.; Prashanth, G.R.; Vemula, P.K. Nanoarchitectonics for free-standing polyelectrolyte multilayers films: Exploring the flipped surfaces. *ChemNanoMat* **2023**, *9*, e202200462. [[CrossRef](#)]

139. Nayak, A.; Unayama, S.; Tai, S.; Tsuruoka, T.; Waser, R.; Aono, M.; Valov, I.; Hasegawa, T. Nanoarchitectonics for controlling the number of dopant atoms in solid electrolyte nanodots. *Adv. Mater.* **2018**, *30*, 1703261. [[CrossRef](#)]
140. Eguchi, M.; Nugraha, A.S.; Rowan, A.E.; Shapter, J.; Yamauchi, Y. Adsorchromism: Molecular nanoarchitectonics at 2D nanosheets—Old chemistry for advanced chromism. *Adv. Sci.* **2021**, *8*, 2100539. [[CrossRef](#)]
141. Yao, B.; Sun, H.; He, Y.; Wang, S.; Liu, X. Recent advances in the photoreactions triggered by porphyrin-based triplet–triplet annihilation upconversion systems: Molecular innovations and nanoarchitectonics. *Int. J. Mol. Sci.* **2022**, *23*, 8041. [[CrossRef](#)]
142. Li, M.; Wu, Z.; Tian, Y.; Pan, F.; Gould, T.; Zhang, S. Nanoarchitectonics of two-dimensional electrochromic materials: Achievements and future challenges. *Adv. Mater. Technol.* **2023**, *8*, 2200917. [[CrossRef](#)]
143. Ogawa, S. Aqueous sugar-based amphiphile systems: Recent advances in phase behavior and nanoarchitectonics. *J. Oleo Sci.* **2023**, *72*, 489–499. [[CrossRef](#)]
144. Qiu, Y.; Zhou, X.; Tang, X.; Hao, Q.; Chen, M. Micro spectrometers based on materials nanoarchitectonics. *Materials* **2023**, *16*, 2253. [[CrossRef](#)] [[PubMed](#)]
145. Zhang, X.; Yang, P. CsPbX<sub>3</sub> (X = Cl, Br, and I) Nanocrystals in substrates toward stable photoluminescence: Nanoarchitectonics, properties, and applications. *Langmuir* **2023**, *39*, 11188–11212. [[CrossRef](#)] [[PubMed](#)]
146. Lun-Fu, A.V.; Bubenchikov, A.M.; Bubenchikov, M.A.; Ovchinnikov, V.A. Numerical simulation of interaction between Kr<sup>+</sup> ion and rotating C<sub>60</sub> fullerene towards for nanoarchitectonics of fullerene materials. *Crystals* **2021**, *11*, 1204. [[CrossRef](#)]
147. Li, X.; Weng, L.; Wang, H.; Wang, X. Nanoarchitectonics of BN/AgNWs/epoxy composites with high thermal conductivity and electrical insulation. *Polymers* **2021**, *13*, 4417. [[CrossRef](#)] [[PubMed](#)]
148. Yang, K.; Qin, G.; Wang, L.; Zhao, M.; Lu, C. Theoretical nanoarchitectonics of GaN nanowires for ultraviolet irradiation-dependent electromechanical properties. *Materials* **2023**, *16*, 1080. [[CrossRef](#)]
149. Tang, R.; Li, G.; Hu, X.; Gao, N.; Li, J.; Huang, K.; Kang, J.; Zhang, R. Micro-nanoarchitectonics of Ga<sub>2</sub>O<sub>3</sub>/GaN core-shell rod arrays for high-performance broadband ultraviolet photodetection. *Crystals* **2023**, *13*, 366. [[CrossRef](#)]
150. Gao, K.; Wu, N.; Ji, B.; Liu, J. A film electrode upon nanoarchitectonics of bacterial cellulose and conductive fabric for forehead electroencephalogram measurement. *Sensors* **2023**, *23*, 7887. [[CrossRef](#)]
151. Howorka, S. DNA Nanoarchitectonics: Assembled DNA at interfaces. *Langmuir* **2013**, *29*, 7344–7353. [[CrossRef](#)]
152. Pandeewar, M.; Senanayak, S.P.; Govindaraju, T. Nanoarchitectonics of small molecule and DNA for ultrasensitive detection of mercury. *ACS Appl. Mater. Interfaces* **2016**, *8*, 30362–30371. [[CrossRef](#)]
153. Zou, Q.; Liu, K.; Abbas, M.; Yan, X. Peptide-modulated self-assembly of chromophores toward biomimetic light-harvesting nanoarchitectonics. *Adv. Mater.* **2016**, *28*, 1031–1043. [[CrossRef](#)] [[PubMed](#)]
154. Komiyama, M.; Yoshimoto, K.; Sisido, M.; Ariga, K. Chemistry can make strict and fuzzy controls for bio-systems: DNA Nanoarchitectonics and cell-macromolecular nanoarchitectonics. *Bull. Chem. Soc. Jpn.* **2017**, *90*, 967–1004. [[CrossRef](#)]
155. Stulz, E. Nanoarchitectonics with porphyrin functionalized DNA. *Acc. Chem. Res.* **2017**, *50*, 823–831. [[CrossRef](#)]
156. Zhang, R.; Wang, Y.; Yang, G. DNA–lysozyme nanoarchitectonics: Quantitative investigation on charge inversion and compaction. *Polymers* **2022**, *14*, 1377. [[CrossRef](#)] [[PubMed](#)]
157. Liu, Q.; Li, H.; Yu, B.; Meng, Z.; Zhang, X.; Li, J.; Zheng, L. DNA-based dissipative assembly toward nanoarchitectonics. *Adv. Funct. Mater.* **2022**, *32*, 2201196. [[CrossRef](#)]
158. Shen, X.; Song, J.; Sevensan, C.; Leong, D.T.; Ariga, K. Bio-interactive nanoarchitectonics with two-dimensional materials and environments. *Sci. Technol. Adv. Mater.* **2022**, *23*, 199–224. [[CrossRef](#)] [[PubMed](#)]
159. Jia, Y.; Yan, X.; Li, J. Schiff base mediated dipeptide assembly toward nanoarchitectonics. *Angew. Chem. Int. Ed.* **2022**, *61*, e202207752. [[CrossRef](#)] [[PubMed](#)]
160. Czarnecka, E.; Nowaczyk, J.; Prochoń, M.; Masek, A. Nanoarchitectonics for biodegradable superabsorbent based on carboxymethyl starch and chitosan cross-linked with vanillin. *Int. J. Mol. Sci.* **2022**, *23*, 5386. [[CrossRef](#)]
161. Kalinova, R.; Mladenova, K.; Petrova, S.; Doumanov, J.; Dimitrov, I. Nanoarchitectonics of spherical nucleic acids with biodegradable polymer cores: Synthesis and evaluation. *Materials* **2022**, *15*, 8917. [[CrossRef](#)]
162. Chang, R.; Zhao, L.; Xing, R.; Li, J.; Yan, X. Functional chromopeptide nanoarchitectonics: Molecular design, self-assembly and biological applications. *Chem. Soc. Rev.* **2023**, *52*, 2688–2712. [[CrossRef](#)] [[PubMed](#)]
163. Li, Z.; Yu, F.; Xu, X.; Wang, T.; Fei, J.; Hao, J.; Li, J. Photozyme-catalyzed ATP generation based on ATP synthase-reconstituted nanoarchitectonics. *J. Am. Chem. Soc.* **2023**, *145*, 20907–20912. [[CrossRef](#)] [[PubMed](#)]
164. Wang, C.; Wang, H.; Na, J.; Yao, Y.; Azhar, A.; Yan, X.; Qi, J.; Yamauchi, Y.; Li, J. 0D–1D hybrid nanoarchitectonics: Tailored design of FeCo@N–C yolk–shell nanoreactors with dual sites for excellent Fenton-like catalysis. *Chem. Sci.* **2021**, *12*, 15418–15422. [[CrossRef](#)] [[PubMed](#)]
165. Huang, C.; Qin, P.; Luo, Y.; Ruan, Q.; Liu, L.; Wu, Y.; Li, Q.; Xu, Y.; Liu, R.; Chu, P.K. Recent progress and perspective of co-balt-based catalysts for water splitting: Design and nanoarchitectonics. *Mater. Today Energy* **2022**, *23*, 100911. [[CrossRef](#)]
166. Chen, G.; Singh, S.K.; Takeyasu, K.; Hill, J.P.; Nakamura, J.; Ariga, K. Versatile nanoarchitectonics of Pt with morphology control of oxygen reduction reaction catalysts. *Sci. Technol. Adv. Mater.* **2022**, *23*, 413–423. [[CrossRef](#)] [[PubMed](#)]
167. Arulraj, A.; Murugesan, P.K.; Rajkumar, C.; Zamorano, A.T.; Mangalaraja, R.V. Nanoarchitectonics of layered metal chalcogenides-based ternary electrocatalyst for water splitting. *Energies* **2023**, *16*, 1669. [[CrossRef](#)]

168. Kumar, A.; Choudhary, P.; Chhabra, T.; Kaur, H.; Kumar, A.; Qamar, M.; Krishnan, V. Frontier nanoarchitectonics of graphitic carbon nitride based plasmonic photocatalysts and photoelectrocatalysts for energy, environment and organic reactions. *Mater. Chem. Front.* **2023**, *7*, 1197–1247. [[CrossRef](#)]
169. Jiang, B.; Guo, Y.; Sun, F.; Wang, S.; Kang, Y.; Xu, X.; Zhao, J.; You, J.; Eguchi, M.; Yamauch, Y.; et al. Nanoarchitectonics of metallene materials for electrocatalysis. *ACS Nano* **2023**, *17*, 13017–13043. [[CrossRef](#)]
170. Lee, G.; Hossain, M.A.; Yoon, M.; Jhung, S.H. Nanoarchitectonics of metal–organic frameworks having hydroxy group for adsorption, catalysis, and sensing. *J. Ind. Eng. Chem.* **2023**, *119*, 181–192. [[CrossRef](#)]
171. Sharma, D.; Choudhary, P.; Kumar, S.; Krishnan, V. Transition metal phosphide nanoarchitectonics for versatile organic catalysis. *Small* **2023**, *19*, 2207053. [[CrossRef](#)] [[PubMed](#)]
172. Wang, Y.; Zhu, S.; He, S.; Lu, J.; Liu, J.; Lu, H.; Song, D.; Luo, Y. Nanoarchitectonics of Ni/CeO<sub>2</sub> catalysts: The effect of pretreatment on the low-temperature steam reforming of glycerol. *Nanomaterials* **2022**, *12*, 816. [[CrossRef](#)] [[PubMed](#)]
173. Cao, H.; Li, H.; Liu, L.; Xue, K.; Niu, X.; Hou, J.; Chen, L. Salt-templated nanoarchitectonics of CoSe<sub>2</sub>-NC nanosheets as an efficient bifunctional oxygen electrocatalyst for water splitting. *Int. J. Mol. Sci.* **2022**, *23*, 5239. [[CrossRef](#)] [[PubMed](#)]
174. Liao, S.; Lin, L.; Huang, J.; Jing, X.; Chen, S.; Li, Q. Microorganism-templated nanoarchitectonics of hollow TiO<sub>2</sub>-SiO<sub>2</sub> microspheres with enhanced photocatalytic activity for degradation of methyl orange. *Nanomaterials* **2022**, *12*, 1606. [[CrossRef](#)] [[PubMed](#)]
175. Lv, Y.; Li, P.; Chen, X.; Wang, D.; Xiao, M.; Song, H.; Gao, J.; Shang, Y. Photo-induced surface oxygen vacancy in hierarchical nanoarchitectonics g-C<sub>3</sub>N<sub>4</sub>/BiOOH to boost photocatalytic CO<sub>2</sub> reduction. *J. Mol. Struct.* **2024**, *1297*, 136961. [[CrossRef](#)]
176. Kalidass, J.; Anandan, S.; Sivasankar, T. Sonoelectrochemical nanoarchitectonics of crystalline mesoporous magnetite @ manganese oxide nanocomposite as an alternate anode material for energy-storage applications. *Crystals* **2023**, *13*, 557. [[CrossRef](#)]
177. Shin, M.; Awasthi, G.P.; Sharma, K.P.; Pandey, P.; Park, M.; Ojha, G.P.; Yu, C. Nanoarchitectonics of three-dimensional carbon nanofiber-supported hollow copper sulfide spheres for asymmetric supercapacitor applications. *Int. J. Mol. Sci.* **2023**, *24*, 9685. [[CrossRef](#)]
178. Ali, N.; Funmilayo, O.R.; Khan, A.; Ali, F.; Bilal, M.; Yang, Y.; Akhter, M.S.; Zhou, C.; Wenjie, Y.; Iqbal, H.M.N. Nanoarchitectonics: Porous hydrogel as bio-sorbent for effective remediation of hazardous contaminants. *J. Inorg. Organomet. Polym.* **2022**, *32*, 3301–3320. [[CrossRef](#)]
179. Ismail, K.S.I.K.; Tajudin, A.A.; Ikeno, S.; Hamzah, A.S.A. Heteroligand nanoarchitectonics of functionalized gold nanoparticle for Hg<sup>2+</sup> detection. *J. Nanopart. Res.* **2022**, *24*, 253. [[CrossRef](#)]
180. Salehipour, M.; Rezaei, S.; Asadi Khalili, H.F.; Motaharian, A.; Manzari, M.M. Nanoarchitectonics of enzyme/metal–organic framework composites for wastewater treatment. *J. Inorg. Organomet. Polym.* **2022**, *32*, 3321–3338. [[CrossRef](#)]
181. Ren, Z.; Yang, X.; Ye, B.; Zhang, W.; Zhao, Z. Biomass-derived mesoporous nanoarchitectonics with magnetic MoS<sub>2</sub> and activated carbon for enhanced adsorption of industrial cationic dye and tetracycline contaminants. *Nano* **2022**, *17*, 2250085. [[CrossRef](#)]
182. Maimaitizi, H.; Abulizi, A.; Talifu, D.; Tursun, Y. Nanoarchitectonics of chlorophyll and Mg co-modified hierarchical BiOCl microsphere as an efficient photocatalyst for CO<sub>2</sub> reduction and ciprofloxacin degradation. *Adv. Powder Technol.* **2022**, *33*, 103562. [[CrossRef](#)]
183. Barreca, D.; Maccato, C. Nanoarchitectonics of metal oxide materials for sustainable technologies and environmental applications. *CrystEngComm* **2023**, *25*, 3968–3987. [[CrossRef](#)]
184. Deng, G.; Xie, L.; Xu, S.; Kang, X.; Ma, J. Fiber nanoarchitectonics for pre-treatments in facile detection of short-chain fatty acids in waste water and faecal samples. *Polymers* **2021**, *13*, 3906. [[CrossRef](#)] [[PubMed](#)]
185. Si, R.; Chen, Y.; Wang, D.; Yu, D.; Ding, Q.; Li, R.; Wu, C. Nanoarchitectonics for high adsorption capacity carboxymethyl cellulose nanofibrils-based adsorbents for efficient Cu<sup>2+</sup> removal. *Nanomaterials* **2022**, *12*, 160. [[CrossRef](#)]
186. Ashraf, I.; Li, R.; Chen, B.; Al-Ansari, N.; Aslam, M.R.; Altaf, A.R.; Elbeltagi, A. Nanoarchitectonics and kinetics insights into fluoride removal from drinking water using magnetic tea biochar. *Int. J. Environ. Res. Public Health* **2022**, *19*, 13092. [[CrossRef](#)]
187. Cheng, Y.; He, J.; Yang, P. Construction of layered SnS<sub>2</sub> and g-C<sub>3</sub>N<sub>4</sub> nanoarchitectonics towards pollution degradation and H<sub>2</sub> generation. *Colloids Surf. A Physicochem. Eng. Asp.* **2024**, *680*, 132678. [[CrossRef](#)]
188. Ishihara, S.; Labuta, J.; Van Rossom, W.; Ishikawa, D.; Minami, K.; Hill, J.P.; Ariga, K. Porphyrin-based sensor nanoarchitectonics in diverse physical detection modes. *Phys. Chem. Chem. Phys.* **2014**, *16*, 9713–9746. [[CrossRef](#)]
189. Komiyama, M.; Mori, T.; Ariga, K. Molecular imprinting: Materials nanoarchitectonics with molecular information. *Bull. Chem. Soc. Jpn.* **2018**, *91*, 1075–1111. [[CrossRef](#)]
190. Jadhav, R.W.; Khobrekar, P.P.; Bugde, S.T.; Bhosale, S.V. Nanoarchitectonics of neomycin-derived fluorescent carbon dots for selective detection of Fe<sup>3+</sup> ions. *Anal. Methods* **2022**, *14*, 3289–3298. [[CrossRef](#)]
191. Ma, K.; Yang, L.; Liu, J.; Liu, J. Electrochemical sensor nanoarchitectonics for sensitive detection of uric acid in human whole blood based on screen-printed carbon electrode equipped with vertically-ordered mesoporous silica-nanochannel film. *Nanomaterials* **2022**, *12*, 1157. [[CrossRef](#)]
192. Joshi, V.; Hussain, S.; Dua, S.; Arora, N.; Mir, S.H.; Rydzek, G.; Senthilkumar, T. Oligomer sensor nanoarchitectonics for “turn-on” fluorescence detection of cholesterol at the nanomolar level. *Molecules* **2022**, *27*, 2856. [[CrossRef](#)]
193. Nishat, Z.S.; Hossain, T.; Islam, M.N.; Phan, H.-P.; Wahab, M.A.; Moni, M.A.; Salomon, C.; Amin, M.A.; Sina, A.A.I.; Hossain, M.S.A.; et al. Hydrogel nanoarchitectonics: An evolving paradigm for ultrasensitive biosensing. *Small* **2022**, *18*, 2107571. [[CrossRef](#)]

194. Vaghasiya, J.V.; Mayorga-Martinez, C.C.; Pumera, M. Wearable sensors for telehealth based on emerging materials and nanoarchitectonics. *npj Flex. Electron.* **2023**, *7*, 26. [[CrossRef](#)]
195. Kim, S.K.; Lee, J.U.; Jeon, M.J.; Kim, S.-K.; Hwang, S.-H.; Hong, M.E.; Sim, S.J. Bio-conjugated nanoarchitectonics with dual-labeled nanoparticles for a colorimetric and fluorescent dual-mode serological lateral flow immunoassay sensor in detection of SARS-CoV-2 in clinical samples. *RSC Adv.* **2023**, *13*, 27225–27232. [[CrossRef](#)]
196. Singh, V.; Thamizhanban, A.; Lalitha, K.; Subbiah, D.K.; Rachamalla, A.K.; Rebaka, V.P.; Banoo, T.; Kumar, Y.; Sridharan, V.; Ahmad, A.; et al. Self-assembling nanoarchitectonics of twisted nanofibers of fluorescent amphiphiles as chemo-resistive sensor for methanol detection. *Gels* **2023**, *9*, 442. [[CrossRef](#)] [[PubMed](#)]
197. Deng, H.-M.; Xiao, M.-J.; Yuan, Y.-L.; Yuan, R.; Chai, Y.-Q. Organic-inorganic cascade-sensitized nanoarchitectonics for photoelectrochemical detection of  $\beta$ 2-MG protein. *Sens. Actuat. B Chem.* **2024**, *398*, 134715. [[CrossRef](#)]
198. Ariga, K.; Ji, Q.; Mori, T.; Naito, M.; Yamauchi, Y.; Abe, H.; Hill, J.P. Enzyme nanoarchitectonics: Organization and device application. *Chem. Soc. Rev.* **2013**, *42*, 6322–6345. [[CrossRef](#)] [[PubMed](#)]
199. Tsuchiya, T.; Nakayama, T.; Ariga, K. Nanoarchitectonics intelligence with atomic switch and neuromorphic network system. *Appl. Phys. Express* **2022**, *15*, 100101. [[CrossRef](#)]
200. Vuk, D.; Radovanović-Perić, F.; Mandić, V.; Lovrinčević, V.; Rath, T.; Panžić, I.; Le-Cunff, J. Synthesis and nanoarchitectonics of novel squaraine derivatives for organic photovoltaic devices. *Nanomaterials* **2022**, *12*, 1206. [[CrossRef](#)]
201. Baek, S.; Kim, S.; Han, S.A.; Kim, Y.H.; Kim, S.; Kim, J.H. Synthesis strategies and nanoarchitectonics for high-performance transition metal dichalcogenide thin film field-effect transistors. *ChemNanoMat* **2023**, *9*, e202300104. [[CrossRef](#)]
202. Zhang, H.; Lin, D.-Q.; Wang, Y.-C.; Li, Z.-X.; Hu, S.; Huang, L.; Zhang, X.-W.; Jin, D.; Sheng, C.-X.; Xu, C.-X.; et al. Hierarchical nanoarchitectonics of ultrathin 2D organic nanosheets for aqueous processed electroluminescent devices. *Small* **2023**, *19*, 2208174. [[CrossRef](#)] [[PubMed](#)]
203. Halder, S.; Chakraborty, C. Fe(II)–Pt(II) based metallo-supramolecular macrocycle nanoarchitectonics for high-performance gel-state electrochromic device. *Dye. Pigment.* **2023**, *212*, 111131. [[CrossRef](#)]
204. Zhou, F.; Zhao, Y.; Fu, F.; Liu, L.; Luo, Z. Thickness nanoarchitectonics with edge-enhanced Raman, polarization Raman, optoelectronic properties of GaS nanosheets devices. *Crystals* **2023**, *13*, 1506. [[CrossRef](#)]
205. Zhao, H.; Li, J.; Sun, W.; He, L.; Li, X.; Jia, X.; Qin, D. Dye-based nanoarchitectonics for the effective bandgap and stability of blue phosphorescent organic light-emitting diodes. *Appl. Phys. A* **2024**, *130*, 53. [[CrossRef](#)]
206. Khan, A.H.; Ghosh, S.; Pradhan, B.; Dalui, A.; Shrestha, L.K.; Acharya, S.; Ariga, K. Two-dimensional (2D) nanomaterials towards electrochemical nanoarchitectonics in energy-related applications. *Bull. Chem. Soc. Jpn.* **2017**, *90*, 627–648. [[CrossRef](#)]
207. Tang, Y.; Yang, C.; Xu, X.; Kang, Y.; Henzie, J.; Que, W.; Yamauchi, Y. MXene nanoarchitectonics: Defect-engineered 2D MXenes towards enhanced electrochemical water splitting. *Adv. Energy Mater.* **2022**, *12*, 2103867. [[CrossRef](#)]
208. Liu, X.; Chen, T.; Xue, Y.; Fan, J.; Shen, S.; Hossain, M.S.A.; Amin, M.A.; Pan, L.; Xu, X.; Yamauchi, Y. Nanoarchitectonics of MXene/semiconductor heterojunctions toward artificial photosynthesis via photocatalytic CO<sub>2</sub> reduction. *Coord. Chem. Rev.* **2022**, *459*, 214440. [[CrossRef](#)]
209. Feng, J.-C.; Xia, H. Application of nanoarchitectonics in moist-electric generation. *Beilstein J. Nanotechnol.* **2022**, *13*, 1185–1200. [[CrossRef](#)]
210. Deepak, D.; Soin, N.; Roy, S.S. Optimizing the efficiency of triboelectric nanogenerators by surface nanoarchitectonics of graphene-based electrodes: A review. *Mater. Today Commun.* **2023**, *34*, 105412. [[CrossRef](#)]
211. Zhang, X.; Yang, P. g-C<sub>3</sub>N<sub>4</sub> Nanosheet nanoarchitectonics: H<sub>2</sub> Generation and CO<sub>2</sub> reduction. *ChemNanoMat* **2023**, *9*, e202300041. [[CrossRef](#)]
212. Ravipati, M.; Badhulika, S. Solvothermal synthesis of hybrid nanoarchitectonics nickel-metal organic framework modified nickel foam as a bifunctional electrocatalyst for direct urea and nitrate fuel cell. *Adv. Powder Technol.* **2023**, *34*, 104087. [[CrossRef](#)]
213. Zhang, X.; Matras-Postolek, K.; Yang, P.; Jiang, S.P. Z-scheme WO<sub>x</sub>/Cu-g-C<sub>3</sub>N<sub>4</sub> heterojunction nanoarchitectonics with promoted charge separation and transfer towards efficient full solar-spectrum photocatalysis. *J. Colloid Interface Sci.* **2023**, *636*, 646–656. [[CrossRef](#)]
214. Kumar, A.V.N.; Yin, S.; Wang, Z.; Qian, X.; Yang, D.; Xu, Y.; Li, X.; Wang, H.; Wang, L. Direct fabrication of bimetallic AuPt nanobrick spherical nanoarchitectonics for the oxygen reduction reaction. *New J. Chem.* **2019**, *43*, 9628–9633. [[CrossRef](#)]
215. Kim, J.; Kim, J.H.; Ariga, K. Redox-active polymers for energy storage nanoarchitectonics. *Joule* **2017**, *1*, 739–768. [[CrossRef](#)]
216. Ezika, A.C.; Sadiku, E.R.; Ray, S.S.; Hamam, Y.; Folurunso, O.; Adekoya, C.J. Emerging advancements in polypyrrole MXene hybrid nanoarchitectonics for capacitive energy storage applications. *J. Inorg. Organomet. Polym.* **2022**, *32*, 1521–1540. [[CrossRef](#)]
217. Yan, D.; Liu, L.; Wang, X.; Xu, K.; Zhong, J. Biomass-derived activated carbon nanoarchitectonics with hibiscus flowers for high-performance supercapacitor electrode applications. *Chem. Eng. Technol.* **2022**, *45*, 649–657. [[CrossRef](#)]
218. Ramadass, K.; Sathish, C.; Singh, G.; Ruban, S.M.; Ruban, A.M.; Bahadur, R.; Kothandam, G.; Belperio, T.; Marsh, J.; Karakoti, A.; et al. Morphologically tunable nanoarchitectonics of mixed kaolin-halloysite derived nitrogen-doped activated nanoporous carbons for supercapacitor and CO<sub>2</sub> capture applications. *Carbon* **2022**, *192*, 133–144. [[CrossRef](#)]
219. Olivares, R.D.O.; Lobato-Peralta, D.R.; Arias, D.M.; Okolie, J.A.; Cuentas-Gallegos, A.K.; Sebastian, P.J.; Mayer, A.R.; Okoye, P.U. Production of nanoarchitectonics corn cob activated carbon as electrode material for enhanced supercapacitor performance. *J. Energy Storage* **2022**, *55*, 105447. [[CrossRef](#)]

220. Li, T.; Dong, H.; Shi, Z.; Yue, H.; Yin, Y.; Li, X.; Zhang, H.; Wu, X.; Li, B.; Yang, S. Composite nanoarchitectonics with CoS<sub>2</sub> nanoparticles embedded in graphene sheets for an anode for lithium-ion batteries. *Nanomaterials* **2022**, *12*, 724. [[CrossRef](#)]
221. Liu, S.; Wei, C.; Wang, H.; Yang, W.; Zhang, J.; Wang, Z.; Zhao, W.; Lee, P.S.; Ai, G. Processable nanoarchitectonics of two-dimensional metallo-supramolecular polymer for electrochromic energy storage devices with high coloration efficiency and stability. *Nano Energy* **2023**, *110*, 108337. [[CrossRef](#)]
222. Zhang, S.; Tamura, A.; Yui, N. Supramolecular nanoarchitectonics of propionylated polyrotaxanes with bulky nitrobenzyl stoppers for light-triggered drug release. *RSC Adv.* **2024**, *14*, 3798–3806. [[CrossRef](#)]
223. Piorecka, K.; Kurjata, J.; Stanczyk, W.A. Nanoarchitectonics: Complexes and conjugates of platinum drugs with silicon containing nanocarriers. An overview. *Int. J. Mol. Sci.* **2021**, *22*, 9264. [[CrossRef](#)]
224. Ferhan, A.R.; Park, S.; Park, H.; Tae, H.; Jackman, J.A.; Cho, N.-J. Lipid nanoparticle technologies for nucleic acid delivery: A nanoarchitectonics perspective. *Adv. Funct. Mater.* **2022**, *32*, 2203669. [[CrossRef](#)]
225. Komiyama, M. Cyclodextrins as eminent constituents in nanoarchitectonics for drug delivery systems. *Beilstein J. Nanotechnol.* **2023**, *14*, 218–232. [[CrossRef](#)] [[PubMed](#)]
226. Aziz, T.; Nadeem, A.A.; Sarwar, A.; Perveen, I.; Hussain, N.; Khan, A.A.; Daudzai, Z.; Cui, H.; Lin, L. Particle nanoarchitectonics for nanomedicine and nanotherapeutic drugs with special emphasis on nasal drugs and aging. *Biomedicines* **2023**, *11*, 354. [[CrossRef](#)] [[PubMed](#)]
227. Jayachandran, P.; Ilango, S.; Suseela, V.; Nirmaladevi, R.; Shaik, M.R.; Khan, M.; Khan, M.; Shaik, B. Green synthesized silver nanoparticle-loaded liposome-based nanoarchitectonics for cancer management: In Vitro drug release analysis. *Biomedicines* **2023**, *11*, 217. [[CrossRef](#)] [[PubMed](#)]
228. Hu, W.; Shi, J.; Lv, W.; Jia, X.; Ariga, K. Regulation of stem cell fate and function by using bioactive materials with nanoarchitectonics for regenerative medicine. *Sci. Technol. Adv. Mater.* **2022**, *23*, 393–412. [[CrossRef](#)] [[PubMed](#)]
229. Tian, B.; Liu, J.; Guo, S.; Li, A.; Wan, J.-B. Macromolecule-based hydrogels nanoarchitectonics with mesenchymal stem cells for regenerative medicine: A review. *Int. J. Biol. Macromol.* **2023**, *243*, 125161. [[CrossRef](#)]
230. Jia, X.; Chen, J.; Lv, W.; Li, H.; Ariga, K. Engineering dynamic and interactive biomaterials using material nanoarchitectonics for modulation of cellular behaviors. *Cell Rep. Phys. Sci.* **2023**, *4*, 101251. [[CrossRef](#)]
231. Yuan, Y.; Chen, L.; Shi, Z.; Chen, J. Micro/nanoarchitectonics of 3D printed scaffolds with excellent biocompatibility prepared using femtosecond laser two-photon polymerization for tissue engineering applications. *Nanomaterials* **2022**, *12*, 391. [[CrossRef](#)]
232. Carrara, S.; Rouvier, F.; Auditto, S.; Brunel, F.; Jeanneau, C.; Camplo, M.; Sergent, M.; About, I.; Bolla, J.-M.; Raimundo, J.-M. Nanoarchitectonics of electrically activable phosphonium self-assembled monolayers to efficiently kill and tackle bacterial infections on demand. *Int. J. Mol. Sci.* **2022**, *23*, 2183. [[CrossRef](#)]
233. Kulikov, O.A.; Zharkov, M.N.; Ageev, V.P.; Yakobson, D.E.; Shlyapkina, V.I.; Zaborovskiy, A.V.; Inchina, V.I.; Balykova, L.A.; Tishin, A.M.; Sukhorukov, G.B.; et al. Magnetic Hyperthermia Nanoarchitectonics via iron oxide nanoparticles stabilised by oleic acid: Anti-tumour efficiency and safety evaluation in animals with transplanted carcinoma. *Int. J. Mol. Sci.* **2022**, *23*, 4234. [[CrossRef](#)]
234. Do, T.T.A.; Wicaksono, K.; Soendoro, A.; Imae, T.; Garcia-Celma, M.J.; Grijalvo, S. Complexation nanoarchitectonics of carbon dots with doxorubicin toward photodynamic anti-cancer therapy. *J. Funct. Biomater.* **2022**, *13*, 219. [[CrossRef](#)]
235. Wu, M.; Liu, J.; Wang, X.; Zeng, H. Recent advances in antimicrobial surfaces via tunable molecular interactions: Nanoarchitectonics and bioengineering applications. *Curr. Opin. Colloid Interface Sci.* **2023**, *66*, 101707. [[CrossRef](#)]
236. Osetrov, K.; Uspenskaya, M.; Zaripova, F.; Olekhovich, R. Nanoarchitectonics of a skin-adhesive hydrogel based on the gelatin resuscitation fluid *Gelatinol*<sup>®</sup>. *Gels* **2023**, *9*, 330. [[CrossRef](#)]
237. Sutrisno, L.; Ariga, K. Pore-engineered nanoarchitectonics for cancer therapy. *NPG Asia Mater.* **2023**, *15*, 21. [[CrossRef](#)]
238. Kumbhar, P.; Kolekar, K.; Khot, C.; Dabhole, S.; Salawi, A.; Sabei, F.A.; Mohite, A.; Kole, K.; Mhatre, S.; Jha, N.K.; et al. Co-crystal nanoarchitectonics as an emerging strategy in attenuating cancer: Fundamentals and applications. *J. Control Release* **2023**, *353*, 1150–1170. [[CrossRef](#)] [[PubMed](#)]
239. Li, B.; Huang, Y.; Zou, Q. Peptide-based nanoarchitectonics for the treatment of liver fibrosis. *ChemBioChem* **2023**, *24*, e202300002. [[CrossRef](#)] [[PubMed](#)]
240. Kim, S.; Baek, S.; Sluyter, R.; Konstantinov, K.; Kim, J.H.; Kim, S.; Kim, Y.H. Wearable and implantable bioelectronics as eco-friendly and patient-friendly integrated nanoarchitectonics for next-generation smart healthcare technology. *EcoMat* **2023**, *5*, e12356. [[CrossRef](#)]
241. Wang, Y.-M.; Xu, Y.; Zhang, X.; Cui, Y.; Liang, Q.; Liu, C.; Wang, X.; Wu, S.; Yang, R. Single Nano-sized metal–organic framework for bio-nanoarchitectonics with in vivo fluorescence imaging and chemo-photodynamic therapy. *Nanomaterials* **2022**, *12*, 287. [[CrossRef](#)]
242. Papadopoulou-Fermeli, N.; Lagopati, N.; Pippa, N.; Sakellis, E.; Boukos, N.; Gorgoulis, V.G.; Gazouli, M.; Pavlatou, E.A. Composite nanoarchitectonics of photoactivated titania-based materials with anticancer properties. *Pharmaceutics* **2023**, *15*, 135. [[CrossRef](#)]
243. Kaganer, V.M.; Möhwald, H.; Dutta, P. Structure and phase transitions in Langmuir monolayers. *Rev. Mod. Phys.* **1999**, *71*, 779–819. [[CrossRef](#)]
244. Ariga, K.; Mori, T.; Hill, J.P. Mechanical control of nanomaterials and nanosystems. *Adv. Mater.* **2012**, *24*, 158–176. [[CrossRef](#)] [[PubMed](#)]

245. Ariga, K.; Yamauchi, Y.; Mori, T.; Hill, J.P. 25th Anniversary article: What can be done with the Langmuir-Blodgett method? Recent developments and its critical role in materials science. *Adv. Mater.* **2013**, *25*, 6477–6512. [[CrossRef](#)]
246. Ariga, K. Don't forget Langmuir-Blodgett films 2020: Interfacial nanoarchitectonics with molecules, materials, and living objects. *Langmuir* **2020**, *36*, 7158–7180. [[CrossRef](#)] [[PubMed](#)]
247. Makiura, R. Creation of metal-organic framework nanosheets by the Langmuir-Blodgett technique. *Coord. Chem. Rev.* **2022**, *469*, 214650. [[CrossRef](#)]
248. Oliveira, O.N., Jr.; Caseli, L.; Ariga, K. The Past and the future of Langmuir and Langmuir-Blodgett films. *Chem. Rev.* **2022**, *122*, 6459–6513. [[CrossRef](#)]
249. Negi, S.; Hamori, M.; Kubo, Y.; Kitagishi, H.; Kano, K. Monolayer formation and chiral recognition of binaphthyl amphiphiles at the air-water interface. *Bull. Chem. Soc. Jpn.* **2023**, *96*, 48–56. [[CrossRef](#)]
250. Decher, G. Fuzzy nanoassemblies: Toward layered polymeric multicomposites. *Science* **1997**, *277*, 1232–1237. [[CrossRef](#)]
251. Rydzek, G.; Ji, Q.; Li, M.; Schaaf, P.; Hill, J.P.; Boulmedais, F.; Ariga, K. Electrochemical nanoarchitectonics and layer-by-layer assembly: From basics to future. *Nano Today* **2015**, *10*, 138–167. [[CrossRef](#)]
252. Richardson, J.J.; Björnmalm, M.; Caruso, F. Technology-driven layer-by-layer assembly of nanofilms. *Science* **2015**, *348*, aaa2491. [[CrossRef](#)] [[PubMed](#)]
253. Akiba, U.; Minaki, D.; Anzai, J. Host-guest chemistry in layer-by-layer assemblies containing calix[n]arenes and cucurbit[n]urils: A Review. *Polymers* **2018**, *10*, 130. [[CrossRef](#)] [[PubMed](#)]
254. Zhang, Z.; Zeng, J.; Groll, J.; Matsusaki, M. Layer-by-layer assembly methods and their biomedical applications. *Biomater. Sci.* **2022**, *10*, 4077–4094. [[CrossRef](#)] [[PubMed](#)]
255. Ariga, K.; Lvov, Y.; Decher, G. There is still plenty of room for layer-by-layer assembly for constructing nanoarchitectonics-based materials and devices. *Phys. Chem. Chem. Phys.* **2022**, *24*, 4097–4115. [[CrossRef](#)] [[PubMed](#)]
256. Wang, C.; Park, M.J.; Yu, H.; Matsuyama, H.; Drioli, E.; Shon, H.K. Recent advances of nanocomposite membranes using layer-by-layer assembly. *J. Membr. Sci.* **2022**, *661*, 120926. [[CrossRef](#)]
257. Simons, K.; Toomre, D. Lipid rafts and signal transduction. *Nat. Rev. Mol. Cell Biol.* **2000**, *1*, 31–39. [[CrossRef](#)] [[PubMed](#)]
258. Chang, L.; Karin, M. Mammalian MAP kinase signalling cascades. *Nature* **2001**, *410*, 37–40. [[CrossRef](#)]
259. Chen, S.; Getter, T.; Salom, D.; Wu, D.; Quetschlich, D.; Chorev, D.S.; Palczewski, K.; Robinson, C.V. Capturing a rhodopsin receptor signalling cascade across a native membrane. *Nature* **2022**, *604*, 384–390. [[CrossRef](#)]
260. Kobashi, J.; Yoshida, H.; Ozaki, M. Planar optics with patterned chiral liquid crystals. *Nat. Photon.* **2016**, *10*, 389–392. [[CrossRef](#)]
261. Kato, T.; Uchida, J.; Ichikawa, T.; Sakamoto, T. Functional liquid crystals towards the next generation of materials. *Angew. Chem. Int. Ed.* **2018**, *57*, 4355–4371. [[CrossRef](#)]
262. Uchida, J.; Soberats, B.; Gupta, M.; Kato, T. Advanced functional liquid crystals. *Adv. Mater.* **2022**, *34*, 2109063. [[CrossRef](#)]
263. Ichimura, K. Photoalignment of liquid-crystal systems. *Chem. Rev.* **2000**, *100*, 1847–1874. [[CrossRef](#)]
264. Ichimura, K.; Suzuki, Y.; Seki, T.; Hosoki, A.; Aoki, K. Reversible change in alignment mode of nematic liquid crystals regulated photochemically by command surfaces modified with an azobenzene monolayer. *Langmuir* **1988**, *4*, 1214–1216. [[CrossRef](#)]
265. Nassrah, A.R.K.; Batkova, M.; Tomašovičová, N.; Tóth-Katona, T. Photoaligning polymeric command Surfaces: Bind, or mix? *Polymers* **2023**, *15*, 4271. [[CrossRef](#)] [[PubMed](#)]
266. Seki, T.; Sakuragi, M.; Kawanishi, Y.; Tamaki, T.; Fukuda, R.; Ichimura, K.; Suzuki, Y. "Command surfaces" of Langmuir-Blodgett films. Photoregulations of liquid crystal alignment by molecularly tailored surface azobenzene layers. *Langmuir* **1993**, *9*, 211–218. [[CrossRef](#)]
267. Kawakami, C.; Hara, M.; Nagano, S.; Seki, T. Induction of highly ordered liquid crystalline phase of an azobenzene side chain polymer by contact with 4'-penty-4-cyanobiphenyl: An in situ study. *Langmuir* **2023**, *39*, 619–626. [[CrossRef](#)] [[PubMed](#)]
268. Thum, M.D.; Ratchford, D.C.; Casalini, R.; Kołacz, J.; Lundin, J.G. Photochemical phase and alignment control of a nematic liquid crystal in core-sheath nanofibers. *J. Mater. Chem. C* **2021**, *9*, 12859–12867. [[CrossRef](#)]
269. Kitagawa, S.; Kitaura, R.; Noro, S. Functional porous coordination polymers. *Angew. Chem. Int. Ed.* **2004**, *43*, 2334–2375. [[CrossRef](#)] [[PubMed](#)]
270. Kambe, T.; Sakamoto, R.; Kusamoto, T.; Pal, T.; Fukui, N.; Hoshiko, K.; Shimojima, T.; Wang, Z.; Hirahara, T.; Ishizaka, K.; et al. Redox control and high conductivity of nickel bis(dithiolene) complex  $\pi$ -nanosheet: A potential organic two-dimensional topological insulator. *J. Am. Chem. Soc.* **2014**, *136*, 14357–14360. [[CrossRef](#)] [[PubMed](#)]
271. Makiura, R.; Motoyama, S.; Umemura, Y.; Yamanaka, H.; Sakata, O.; Kitagawa, H. Surface nano-architecture of a metal-organic framework. *Nat. Mater.* **2010**, *9*, 565–571. [[CrossRef](#)]
272. Kitao, T.; Zhang, Y.; Kitagawa, S.; Wan, B.; Uemura, T. Hybridization of MOFs and polymers. *Chem. Soc. Rev.* **2017**, *46*, 3108–3133. [[CrossRef](#)]
273. Bieniek, A.; Terzyk, A.P.; Wiśniewski, M.; Roszek, K.; Kowalczyk, P.; Sarkisov, L.; Keskin, S.; Kaneko, K. MOF materials as therapeutic agents, drug carriers, imaging agents and biosensors in cancer biomedicine: Recent advances and perspectives. *Prog. Mater. Sci.* **2021**, *117*, 100743. [[CrossRef](#)]
274. Kim, M.; Xin, R.; Earnshaw, J.; Tang, J.; Hill, J.P.; Ashok, A.; Nanjundan, A.K.; Kim, J.; Young, C.; Sugahara, Y.; et al. MOF-derived nanoporous carbons with diverse tunable nanoarchitectures. *Nat. Protoc.* **2022**, *17*, 2990–3027. [[CrossRef](#)]
275. Sánchez-González, E.; Tsang, M.Y.; Troyano, J.; Craig, G.A.; Furukawa, S. Assembling metal-organic cages as porous materials. *Chem. Soc. Rev.* **2022**, *51*, 4876–4889. [[CrossRef](#)] [[PubMed](#)]

276. Sarango-Ramírez, M.K.; Donoshita, M.; Yoshida, Y.; Lim, D.-W.; Kitagawa, H. Cooperative proton and Li-ion conduction in a 2D-layered MOF via mechanical insertion of lithium halides. *Angew. Chem. Int. Ed.* **2023**, *62*, e202301284. [[CrossRef](#)]
277. Fujiwara, A.; Wang, J.; Hiraide, S.; Götz, A.; Miyahara, M.T.; Hartmann, M.; Apeleo Zubiri, B.; Spiecker, E.; Vogel, N.; Watanabe, S. Fast gas-adsorption kinetics in supraparticle-based MOF packings with hierarchical porosity. *Adv. Mater.* **2023**, *35*, e2305980. [[CrossRef](#)] [[PubMed](#)]
278. Hung, H.-L.; Iizuka, T.; Deng, X.; Lyu, Q.; Hsu, C.-H.; Oe, N.; Lin, L.-C.; Hosono, N.; Kang, D.-Y. Engineering gas separation property of metal–organic framework membranes via polymer insertion. *Sep. Purif. Technol.* **2023**, *310*, 123115. [[CrossRef](#)]
279. Ohata, T.; Tachimoto, K.; Takeno, K.J.; Nomoto, A.; Watanabe, T.; Hirosawa, I.; Makiura, R. Influence of the solvent on the assembly of Ni<sub>3</sub>(hexaiminotriphenylene)<sub>2</sub> metal–organic framework nanosheets at the air/liquid interface. *Bull. Chem. Soc. Jpn.* **2023**, *96*, 274–282. [[CrossRef](#)]
280. Dey, K.; Pal, M.; Rou, K.C.; Kunjattu, H.S.; Das, A.; Mukherjee, R.; Kharul, U.K.; Banerjee, R. Selective molecular separation by interfacially crystallized covalent organic framework thin films. *J. Am. Chem. Soc.* **2017**, *139*, 13083–13091. [[CrossRef](#)]
281. Sun, K.; Wang, C.; Dong, Y.; Guo, P.; Cheng, P.; Fu, Y.; Liu, D.; He, D.; Das, S.; Negishi, Y. Ion-selective covalent organic framework membranes as a catalytic polysulfide trap to arrest the redox shuttle effect in lithium–sulfur batteries. *ACS Appl. Mater. Interfaces* **2022**, *14*, 4079–4090. [[CrossRef](#)] [[PubMed](#)]
282. Zhao, Y.; Das, S.; Sekine, T.; Mabuchi, H.; Irie, T.; Sakai, J.; Wen, D.; Zhu, W.; Ben, T.; Negishi, Y. Record ultralarge-pores, low density three-dimensional covalent organic Framework for controlled drug delivery. *Angew. Chem. Int. Ed.* **2023**, *62*, e202300172. [[CrossRef](#)]
283. Huang, L.; Yang, J.; Asakura, Y.; Shuai, Q.; Yamauchi, Y. Nanoarchitectonics of hollow covalent organic frameworks: Synthesis and applications. *ACS Nano* **2023**, *17*, 8918–8934. [[CrossRef](#)]
284. Du, J.; Sun, Q.; He, W.; Liu, L.; Song, Z.; Yao, A.; Ma, J.; Cao, D.; Hassan, S.U.; Guan, J.; et al. A 2D soft covalent organic framework membrane prepared via a molecular bridge. *Adv. Mater.* **2023**, *35*, 2300975. [[CrossRef](#)]
285. Jin, F.; Wang, T.; Zheng, H.; Lin, E.; Zheng, Y.; Hao, L.; Wang, T.; Chen, Y.; Cheng, P.; Yu, K.; et al. Bottom-up synthesis of covalent organic Frameworks with quasi-three-dimensional integrated architecture via interlayer cross-linking. *J. Am. Chem. Soc.* **2023**, *145*, 6507–6515. [[CrossRef](#)]
286. Xiao, Y.; Ling, Y.; Wang, K.; Ren, S.; Ma, Y.; Li, L. Constructing a 3D covalent organic framework from 2D hcb nets through inclined interpenetration. *J. Am. Chem. Soc.* **2023**, *145*, 13537–13541. [[CrossRef](#)]
287. Cheng, Y.; Xin, J.; Xiao, L.; Wang, X.; Zhou, X.; Li, D.; Gui, B.; Sun, J.; Wang, C. A Fluorescent three-dimensional covalent organic framework formed by the entanglement of two-dimensional sheets. *J. Am. Chem. Soc.* **2023**, *145*, 18737–18741. [[CrossRef](#)] [[PubMed](#)]
288. Parvin, N.; Mandal, T.K.; Joo, S.W. Development of pseudo 3D covalent organic framework nanosheets for sensitive and selective biomolecule detection of infectious disease. *J. Mater. Chem. C* **2023**, *11*, 16398–16410. [[CrossRef](#)]
289. Gutiérrez-Tarriño, S.; Olloqui-Sariego, J.L.; Calvente, J.J.; Espallargas, G.M.; Rey, F.; Corma, A.; Oña-Burgos, P. Cobalt metal–organic framework based on layered double nanosheets for enhanced electrocatalytic water oxidation in neutral media. *J. Am. Chem. Soc.* **2020**, *142*, 19198–19208. [[CrossRef](#)]
290. Zou, Y.; Liu, C.; Zhang, C.; Yuan, L.; Li, J.; Bao, T.; Wei, G.; Zou, J.; Yu, C. Epitaxial growth of metal-organic framework nanosheets into single-crystalline orthogonal arrays. *Nat. Commun.* **2023**, *14*, 5780. [[CrossRef](#)]
291. Li, X.; Jiang, G.; Jian, M.; Zhao, C.; Hou, J.; Thornton, A.W.; Zhang, X.; Liu, J.Z.; Freeman, B.D.; Wang, H.; et al. Construction of angstrom-scale ion channels with versatile pore configurations and sizes by metal-organic frameworks. *Nat. Commun.* **2021**, *14*, 286. [[CrossRef](#)]
292. Choi, J.Y.; Flood, J.; Stodolka, M.; Pham, H.T.B.; Park, J. From 2D to 3D: Postsynthetic pillar insertion in electrically conductive MOF. *ACS Nano* **2022**, *16*, 3145–3151. [[CrossRef](#)]
293. Wee, L.H.; Meledina, M.; Turner, S.; Van Tendeloo, G.; Zhang, K.; Rodriguez-Albelo, L.M.; Masala, A.; Bordiga, S.; Jiang, J.; Navarro, J.A.R.; et al. 1D-2D-3D Transformation synthesis of hierarchical metal–organic framework adsorbent for multicomponent alkane separation. *J. Am. Chem. Soc.* **2017**, *139*, 819–828. [[CrossRef](#)]
294. Wang, Y.; Zhang, Z.; Li, J.; Yuan, Y.; Yang, J.; Xu, W.; An, P.; Xi, S.; Guo, J.; Liu, B.; et al. Two-dimensional-on-three-dimensional metal-organic frameworks for photocatalytic H<sub>2</sub> production. *Angew. Chem. Int. Ed.* **2022**, *61*, e202211031. [[CrossRef](#)]
295. Lei, Q.; Sun, Y.; Huang, J.; Liu, W.; Zhan, X.; Yin, W.; Guo, S.; Sinelshchikova, A.; Brinker, C.J.; He, Z.; et al. Dimensional reduction of metal–organic frameworks for enhanced cryopreservation of red blood cells. *Angew. Chem. Int. Ed.* **2023**, *62*, e202217374. [[CrossRef](#)]
296. Jia, X.; Minami, K.; Uto, K.; Chang, A.C.; Hill, J.P.; Nakanishi, J.; Ariga, K. Adaptive liquid interfacially assembled protein nanosheets for guiding mesenchymal stem cell fate. *Adv. Mater.* **2020**, *32*, 1905942. [[CrossRef](#)] [[PubMed](#)]
297. Jia, X.; Song, J.; Lv, W.; Hill, J.P.; Nakanishi, J.; Ariga, K. Adaptive liquid interfaces induce neuronal differentiation of mesenchymal stem cells through lipid raft assembly. *Nat. Commun.* **2022**, *13*, 3110. [[CrossRef](#)] [[PubMed](#)]
298. Chrysanthou, A.; Bosch-Fortea, M.; Gautrot, J.E. Co-surfactant-free bioactive protein nanosheets for the stabilization of bioemulsions enabling adherent cell expansion. *Biomacromolecules* **2023**, *24*, 4465–4477. [[CrossRef](#)] [[PubMed](#)]
299. Kong, D.; Megone, W.; Nguyen, K.D.Q.; Cio, S.D.; Ramstedt, M.; Gautrot, J.E. Protein nanosheet mechanics controls cell adhesion and expansion on low-viscosity liquids. *Nano Lett.* **2018**, *18*, 1946–1951. [[CrossRef](#)] [[PubMed](#)]

300. Kong, D.; Peng, L.; Cio, S.D.; Novak, P.; Gautrot, J.E. Stem cell expansion and fate decision on liquid substrates are regulated by self-assembled nanosheets. *ACS Nano* **2018**, *12*, 9206–9213. [[CrossRef](#)] [[PubMed](#)]
301. Miyazawa, K.; Kuwasaki, Y.; Obayashi, A.; Kuwabara, M. C<sub>60</sub> nanowhiskers formed by the liquid–liquid interfacial precipitation method. *J. Mater. Res.* **2002**, *17*, 83–88. [[CrossRef](#)]
302. Sathish, M.; Miyazawa, K. Size-tunable hexagonal fullerene (C<sub>60</sub>) nanosheets at the liquid–liquid interface. *J. Am. Chem. Soc.* **2007**, *129*, 13816–13817. [[CrossRef](#)]
303. Park, C.; Yoon, E.; Kawano, M.; Joo, T.; Choi, H.C. Self-crystallization of C<sub>70</sub> cubes and remarkable enhancement of photoluminescence. *Angew. Chem. Int. Ed.* **2010**, *49*, 9670–9675. [[CrossRef](#)] [[PubMed](#)]
304. Nakanishi, W.; Minami, K.; Shrestha, L.K.; Ji, Q.; Hill, J.P.; Ariga, K. Bioactive nanocarbon assemblies: Nanoarchitectonics and applications. *Nano Today* **2014**, *9*, 378–394. [[CrossRef](#)]
305. Miyazawa, K. Synthesis of fullerene nanowhiskers using the liquid–liquid interfacial precipitation method and their mechanical, electrical and superconducting properties. *Sci. Technol. Adv. Mater.* **2015**, *16*, 013502. [[CrossRef](#)] [[PubMed](#)]
306. Kim, J.; Park, C.; Choi, H.C. Selective growth of a C<sub>70</sub> crystal in a mixed solvent system: From cube to tube. *Chem. Mater.* **2015**, *27*, 2408–2413. [[CrossRef](#)]
307. Song, J.; Murata, T.; Tsai, K.-C.; Jia, X.; Sciortino, F.; Ma, R.; Yamauchi, Y.; Hill, J.P.; Shrestha, L.K.; Ariga, K. Fullerphene nanosheets: A bottom-Up 2D material for single-carbon-atom-level molecular discrimination. *Adv. Mater. Interfaces* **2022**, *9*, 2102241. [[CrossRef](#)]
308. Koya, I.; Yokoyama, Y.; Sakka, T.; Nishi, N. Formation of Au nanofiber/fullerene nanowhisker 1D/1D composites via reductive deposition at the interface between an ionic liquid and water. *Chem. Lett.* **2022**, *51*, 643–645. [[CrossRef](#)]
309. Chen, G.; Sciortino, F.; Takeyasu, K.; Nakamura, J.; Hill, J.P.; Shrestha, L.K.; Ariga, K. Hollow spherical fullerene obtained by kinetically controlled liquid-liquid interfacial precipitation. *Chem. Asian J.* **2022**, *17*, e20220075. [[CrossRef](#)]
310. Minami, K.; Kasuya, Y.; Yamazaki, Y.; Ji, Q.; Nakanishi, W.; Hill, J.P.; Sakai, H.; Ariga, K. Highly ordered 1D fullerene crystals for concurrent control of macroscopic cellular orientation and differentiation toward large-scale tissue engineering. *Adv. Mater.* **2015**, *27*, 4020–4026. [[CrossRef](#)]
311. Song, J.; Jia, X.; Minami, K.; Hill, J.P.; Nakanishi, J.; Shrestha, L.K.; Ariga, K. Large-area aligned fullerene nanocrystal scaffolds as culture substrates for enhancing mesenchymal stem cell self-renewal and multipotency. *ACS Appl. Nano Mater.* **2020**, *3*, 6497–6506. [[CrossRef](#)]
312. dos Santos, R.B.; Rivelino, R.; Gueorguiev, G.K.; Kakanakova-Georgieva, A. Exploring 2D structures of indium oxide of different stoichiometry. *CrystEngComm* **2021**, *23*, 6661–6667. [[CrossRef](#)]
313. Sangiovanni, D.G.; Faccio, R.; Gueorguiev, G.K.; Kakanakova-Georgieva, A. Discovering atomistic pathways for supply of metal atoms from methyl-based precursors to graphene surface. *Phys. Chem. Chem. Phys.* **2023**, *25*, 829–837. [[CrossRef](#)]
314. Mahmood, A.; Sandali, Y.; Wang, J.-L. Easy and fast prediction of green solvents for small molecule donor-based organic solar cells through machine learning. *Phys. Chem. Chem. Phys.* **2023**, *25*, 10417–10426. [[CrossRef](#)]
315. Yang, C.; Zhang, D.; Wang, D.; Luan, H.; Chen, X.; Yan, W. In Situ polymerized MXene/polypyrrole/hydroxyethyl cellulose-based flexible strain sensor enabled by machine learning for handwriting recognition. *ACS Appl. Mater. Interfaces* **2023**, *15*, 5811–5821. [[CrossRef](#)]
316. Hangai, Y.; Ozawa, S.; Okada, K.; Tanaka, Y.; Amagai, K.; Suzuki, R. Machine learning estimation of plateau stress of aluminum foam using X-ray computed tomography images. *Materials* **2023**, *16*, 1894. [[CrossRef](#)]
317. Agrawala, A.; Choudhary, A. Perspective: Materials informatics and big data: Realization of the “fourth paradigm” of science in materials science. *APL Mater.* **2016**, *4*, 053208. [[CrossRef](#)]
318. Ramprasad, R.; Batra, R.; Pilia, G.; Mannodi-Kanakkithodi, A.; Kim, C. Machine learning in materials informatics: Recent applications and prospects. *NPJ Comput. Mater.* **2017**, *3*, 54. [[CrossRef](#)]
319. Hatakeyama-Sato, K.; Umeki, M.; Adachi, H.; Kuwata, N.; Hasegawa, G.; Oyaizu, K. Exploration of organic superionic glassy conductors by process and materials informatics with lossless graph database. *npj Comput. Mater.* **2022**, *8*, 170. [[CrossRef](#)]
320. Chaikittisilp, W.; Yamauchi, Y.; Ariga, K. Material evolution with nanotechnology, nanoarchitectonics, and materials informatics: What will be the next paradigm shift in nanoporous materials? *Adv. Mater.* **2022**, *34*, 2107212. [[CrossRef](#)] [[PubMed](#)]
321. Oviedo, L.R.; Oviedo, V.R.; Martins, M.O.; Fagan, S.B.; da Silva, W.L. Nanoarchitectonics: The role of artificial intelligence in the design and application of nanoarchitectures. *J. Nanopart. Res.* **2022**, *24*, 157. [[CrossRef](#)]

**Disclaimer/Publisher’s Note:** The statements, opinions and data contained in all publications are solely those of the individual author(s) and contributor(s) and not of MDPI and/or the editor(s). MDPI and/or the editor(s) disclaim responsibility for any injury to people or property resulting from any ideas, methods, instructions or products referred to in the content.